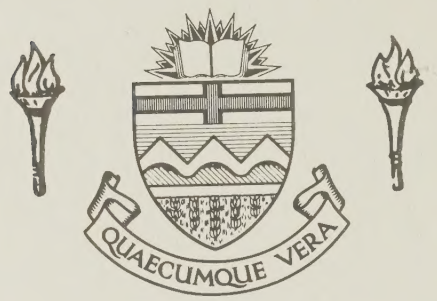


For Reference

NOT TO BE TAKEN FROM THIS ROOM

Ex LIBRIS
UNIVERSITATIS
ALBERTAEISIS





Digitized by the Internet Archive
in 2022 with funding from
University of Alberta Library

<https://archive.org/details/Millar1978>

THE UNIVERSITY OF ALBERTA

NUCLEAR MAGNETIC RESONANCE STUDIES OF THE SOLUTION CHEMISTRY
OF TRIMETHYLLLEAD COMPLEXES

by



EMIKO KANEKO MILLAR

A THESIS

SUBMITTED TO THE FACULTY OF GRADUATE STUDIES AND
RESEARCH IN PARTIAL FULFILMENT OF THE REQUIREMENTS
FOR THE DEGREE OF MASTER OF SCIENCE

DEPARTMENT OF CHEMISTRY

EDMONTON, ALBERTA

FALL, 1978

To George

ABSTRACT

The aqueous solution chemistry of trimethyllead (IV) species and of the trimethyllead complexes of selected inorganic anions has been investigated by proton magnetic resonance spectroscopy. Equilibrium constants for the reaction of $(\text{CH}_3)_3\text{Pb}^+$ with hydroxide ion to form $(\text{CH}_3)_3\text{PbOH}$ and $((\text{CH}_3)_3\text{Pb})_2\text{OH}^+$ have been determined from the pH dependence of the chemical shift of the methyl protons of trimethyllead. Formation constants were also determined for the sulfite, selenite, thiosulfate, thiocyanate, phosphate, carbonate, iodide, bromide, and chloride complexes from the pH dependence of the chemical shift of the methyl protons of trimethyllead in solutions containing both trimethyllead and ligand. The lead - 207 - proton coupling constant was found to be insensitive to complexation. The formation constants are in general fairly small and the extent to which complexes form is strongly dependent on pH. At high pH, $(\text{CH}_3)_3\text{PbOH}$ forms while at low pH, protonation of those ligands which are the conjugate bases of weak acids competes with complex formation. There is no indication of high selectivity in the binding of trimethyllead by a particular ligand type, and calculations indicate that any trimethyllead in biological fluids is likely to be distributed among a variety of ligands, including chloride which forms uncharged and presumably lipid soluble $(\text{CH}_3)_3\text{PbCl}$.

ACKNOWLEDGEMENTS

I wish to express my thanks to my supervisor, Dr. D. L. Rabenstein, for his guidance throughout the duration of this research.

I would also like to thank Dr. C. A. Evans for his continual advice and help.

I sincerely acknowledge the unending support and encouragement from my husband, parents and colleagues in the research group.

Special thanks goes to Mrs. J. Jorgensen for an excellent typing job.

The financial support of a Water Resources Research Support Program Grant from the Inland Waters Directorate, Environment Canada and the University of Alberta is gratefully acknowledged.

TABLE OF CONTENTS

CHAPTER	PAGE
LIST OF TABLES.....	ix
LIST OF FIGURES.....	x
NUCLEAR MAGNETIC RESONANCE STUDIES OF THE SOLUTION CHEMISTRY OF TRIMETHYLLEAD COMPLEXES	
I. INTRODUCTION.....	1
A. Sources and Transformations of Organolead Compounds in the Environment.....	1
B. Lead Poisoning.....	4
C. Coordination Chemistry of Trimethyllead.....	6
D. The Present Study.....	11
II. EXPERIMENTAL.....	12
A. Chemicals.....	12
B. Preparation and Standardization of Tri- methyllead Solutions.....	13
C. Preparation and Standardization of Ligand Solutions.....	15
D. pH Measurements.....	17
E. Proton Nuclear Magnetic Resonance Measurements.....	17
F. Solutions for Nuclear Magnetic Resonance Measurements.....	18
G. Determination of Formation Constants by NMR Spectroscopy.....	21
H. Determination of Acid Dissociation Constants of Selected Ligands by pH Titration.....	23
III. TRIMETHYLLEAD SPECIES AND EQUILIBRIA IN AQUEOUS SOLUTION.....	25
Results and Discussion.....	25

CHAPTER	PAGE
IV. TRIMETHYLLEAD COMPLEXES OF SELECTED INORGANIC ANIONS	40
A. Results.....	40
1. The Sulfite and Selenite Complexes of Trimethyllead.....	40
2. The Thiosulfate Complex of Trimethyl-lead.....	52
3. The Thiocyanate Complex of Trimethyl-lead.....	56
4. The Sulfide Complex of Trimethyllead.....	61
5. The Phosphate Complex of Trimethyl-lead.....	64
6. The Carbonate Complex of Trimethyl-lead.....	67
7. The Iodide, Bromide, Chloride, and Fluoride Complexes of Trimethyllead.....	70
B. Discussion.....	74
BIBLIOGRAPHY.....	86

LIST OF TABLES

Table	Description	Page
1	Chemical Shift Data and Calculated Values for $\log K_1$ for Trimethyllead (5.00×10^{-3} M).....	30
2	Chemical Shift Data and Calculated Values for $\log K_1$ for Trimethyllead (0.185 M).....	32
3	Summary of Acid Dissociation Constants and Formation Constants of the Trimethyllead and the Methylmercury Complexes of Selected Inorganic Ligands, and the Trimethyllead Chemical Shifts of Their Trimethyllead Complexes.....	53

LIST OF FIGURES

Figure	Page
1. Proton NMR spectrum of the methyl groups of trimethyllead in 0.140 M solution.	26
2. pH dependence of the chemical shift of the methyl protons of trimethyllead in an aqueous solution containing 5.00×10^{-3} M trimethyllead perchlorate.	28
3. pH dependence of the trimethyllead species distribution in a 0.200 M aqueous solution calculated using K_1 and K_2 as in the text.	37
4. pH dependence of the trimethyllead species distribution in a 5.00×10^{-3} M aqueous solution calculated using K_1 and K_2 as in the text.	38
5. pH dependence of the chemical shift of the methyl protons of trimethyllead in an aqueous solution containing 5.00×10^{-3} M trimethyllead perchlorate (open points) and in an aqueous solution containing 5.00×10^{-3} M trimethyllead perchlorate and 0.0612 M sodium sulfite (solid points).	42
6. pH dependence of the chemical shift of the methyl protons of trimethyllead in an aqueous solution containing 5.00×10^{-3} M trimethyllead perchlorate (open points) and in an aqueous solution containing 4.83×10^{-3} M trimethyllead perchlorate and 0.0504 M sodium selenite (solid points).	50

7. pH dependence of the chemical shift of the methyl protons of trimethyllead in an aqueous solution containing 5.00×10^{-3} M trimethyllead perchlorate (open points) and in an aqueous solution containing 5.00×10^{-3} M trimethyllead perchlorate and 0.0503 M sodium thiosulfate (solid points). 55
8. Mole ratio dependence of the chemical shift of the methyl protons of trimethyllead in aqueous solutions having sodium thiocyanate and trimethyllead perchlorate ratios between 0-300 at pH 5.00. Trimethyllead perchlorate = 5.00×10^{-3} M, Ionic strength = 1.5 M (NaClO_4 as required). 58
9. pH dependence of the chemical shift of the methyl protons of trimethyllead in an aqueous solution containing 5.00×10^{-3} M trimethyllead perchlorate (open points) and in an aqueous solution containing 5.03×10^{-3} M trimethyllead perchlorate and 0.0124 M sodium sulfide (solid points). 63
10. pH dependence of the chemical shift of the methyl protons of trimethyllead in an aqueous solution containing 5.00×10^{-3} M trimethyllead perchlorate (open points) and in an aqueous solution containing 5.00×10^{-3} M trimethyllead perchlorate and 0.0135 M di-sodium hydrogen orthophosphate (solid points). 65

Figure	Page
11. pH dependence of the chemical shift of the methyl protons of trimethyllead in an aqueous solution containing 5.00×10^{-3} M trimethyllead perchlorate (open points) and in an aqueous solution containing 5.03×10^{-3} M trimethyllead perchlorate and 0.0650 M sodium carbonate (solid points).	68
12. The chemical shift of the methyl protons of trimethyllead in aqueous solutions containing 2.00×10^{-3} M trimethyllead perchlorate and sodium halide as a function of the ligand-to-trimethyllead ratio at pH 4.00. Sodium iodide (O), sodium bromide (●), and sodium chloride (Δ).	72
13. pH dependence of the trimethyllead species distribution in an aqueous solution containing 5.00×10^{-3} M trimethyllead perchlorate and 0.0500 M sodium phosphate. $(\text{CH}_3)_3\text{Pb}^+$ (a), $(\text{CH}_3)_3-\text{PbOH}$ (b), $(\text{CH}_3)_3\text{Pb}(\text{HPO}_4)^-$ (c), and $((\text{CH}_3)_3\text{Pb})_2\text{OH}^+$ (d).	77
14. pH dependence of the trimethyllead species distribution in an aqueous solution containing 5.00×10^{-3} M trimethyllead perchlorate and 0.0500 M sodium thiosulfate. $(\text{CH}_3)_3\text{Pb}^+$ (a), $(\text{CH}_3)_3\text{PbOH}$ (b), $(\text{CH}_3)_3\text{Pb}(\text{S}_2\text{O}_3)^-$ (c), and $((\text{CH}_3)_3-\text{Pb})_2\text{OH}^+$ (d).	78

Figure	Page
15. pH dependence of the trimethyllead species distribution in an aqueous solution containing 5.00×10^{-3} M trimethyllead perchlorate and 0.0500 M sodium chloride. $(\text{CH}_3)_3\text{Pb}^+$ (a), $(\text{CH}_3)_3\text{PbOH}$ (b), $(\text{CH}_3)_3\text{PbCl}$ (c), and $((\text{CH}_3)_3\text{Pb})_2\text{OH}^+$ (d).	79
16. pH dependence of the distribution of trimethyllead among its various forms in an aqueous solution containing trimethyllead perchlorate, 2-mercaptopropanol and sodium phosphate, each at a total concentration of 5.00×10^{-3} M. $(\text{CH}_3)_3\text{Pb}^+$ (a), $(\text{CH}_3)_3\text{Pb}(\text{SCH}_2\text{CH}_2\text{OH})$ (b), $(\text{CH}_3)_3\text{PbOH}$ (c), $(\text{CH}_3)_3\text{Pb}(\text{HPO}_4)^-$ (d), and $((\text{CH}_3)_3\text{Pb})_2\text{SCH}_2\text{CH}_2\text{OH}^+$ (e).	82
17. pH dependence of the distribution of trimethyllead among its various forms in an aqueous solution containing trimethyllead perchlorate, 2-mercaptopropanol and sodium phosphate, each at a total concentration of 0.100 M. $(\text{CH}_3)_3\text{Pb}^+$ (a), $(\text{CH}_3)_3\text{Pb}(\text{SCH}_2\text{CH}_2\text{OH})$ (b), $(\text{CH}_3)_3\text{PbOH}$ (c), $(\text{CH}_3)_3\text{Pb}(\text{HPO}_4)^-$ (d), and $((\text{CH}_3)_3\text{Pb})_2\text{SCH}_2\text{CH}_2\text{OH}^+$ (e).	83
18. pH dependence of the distribution of trimethyllead among its various forms in an aqueous solution containing 5.00×10^{-3} M trimethyllead perchlorate and 2-mercaptopropanol and 0.100 M sodium chloride. $(\text{CH}_3)_3\text{Pb}^+$ (a), $(\text{CH}_3)_3\text{Pb}(\text{SCH}_2\text{CH}_2\text{OH})$ (b), $(\text{CH}_3)_3\text{PbOH}$ (c), $(\text{CH}_3)_3\text{PbCl}$ (d), and $((\text{CH}_3)_3\text{Pb})_2\text{SCH}_2\text{CH}_2\text{OH}^+$ (e).	84

CHAPTER I
INTRODUCTION

Tetraorganolead(IV) compounds are cleaved in the body to form triorganolead(IV) species (1,2) which are in general easily transported around the body in contrast to inorganic lead which often forms an insoluble salt. In addition methylated lead compounds have been shown to be produced by lake sediments (3), constituting another possible source for organolead poisoning. Despite these facts little is known about the coordination chemistry of organolead in aqueous solution and no effective drugs are known for organolead poisoning.

In this thesis the results of a study of the aqueous solution chemistry of trimethyllead(IV) and of trimethyllead(IV) complexes of selected inorganic ligands are reported. The research described in this thesis is part of a program to provide information about the aqueous solution chemistry of trimethyllead(IV) and its complexes.

A. Sources and Transformations of Organolead compounds in the Environment.

Lead is one of the most toxic metals found in the environment and is of great concern because of its widespread occurrence in nature, but its fate after dispersion by man's activities is largely unknown. Most of the lead discharged into the environment is in the form of

inorganic salts or the metal itself. Some ten percent of the lead used industrially is manufactured into organolead compounds which are almost entirely discharged into the atmosphere because of its use as an antiknock compound in fuel for internal combustion engines (4). In addition several new uses for organolead compounds have been discovered recently. These include the use of triorganolead (particularly triphenyllead) salts as biocidal agents, the use of monoaryllead compounds as catalysts in polymer- and gas-forming reactions, and the use of various triorganolead compounds as antiwear additives to lubricants (4). At present, the use of tetraethyl- and tetramethylead accounts for considerably more than eighty percent of all industrial applications of organometallic compounds.

Until a few years ago, nothing was known about the existence of organic forms of lead in the environment as a result of biotransformation (5). Recently, however, it has been discovered by Wong, Chau and Luxon that certain inorganic and organic lead compounds can be converted to volatile tetramethylead by microorganisms in lake sediments (3). The pathways for the biological conversion of lead are not well understood. It is apparent that the conversion of inorganic lead to organic lead is a difficult process. On the other hand, trimethyllead salts are readily converted to tetramethylead by

microorganisms in lake water or a nutrient medium, with or without the sediment, and in the presence, or the absence, of light. Following this report of methylation of lead by anaerobic microorganisms, Jarvie, Markall and Potter investigated the formation of organolead compounds in aqueous systems (6). Alkylation of $Pb(NO_3)_2$ in sediment systems could not be detected in their study. Their results suggest that the main reaction producing tetraalkyllead from trialkyllead salts in anaerobic systems is the conversion of the trialkyllead salt to the sulphide, and the subsequent decomposition of the trialkyllead sulphide $(R_3Pb)_2S$ to form the tetraalkyllead. The absence of methyl triethyllead when triethyllead chloride is added to sediment shows that no direct methylation is occurring in this case. In aqueous solution, methyllead compounds $(CH_3)_2PbX_2$ and $(CH_3)_3PbX$ (X = anion) redistribute according to



Reaction 2 is much faster than 1 (7,8) and the rate of both reactions depends on the nature of X . $(CH_3)_3PbX$ is relatively stable at room temperature. The overall stoichiometry of its decomposition can be described by

reaction 3. Schmidt and Huber (9) extended these observations, and conclude that, besides the formation of $(\text{CH}_3)_4\text{Pb}$ by redistribution according to reaction 1, biological alkylation of Pb^{2+} must be considered as another source for $(\text{CH}_3)_4\text{Pb}$. In view of the high redox potential, +1.46 volts, for the lead(IV)/lead(II) couple and the instability of monoalkyllead compounds in aqueous solution (10) it is difficult to explain the conversion of inorganic lead(II) to tetramethyllead(IV) observed by Wong, Chau and Luxon (3), and Schmidt and Huber (9).

B. Lead poisoning.

Lead poisoning is one of the commonest of occupational diseases. Penetration of the body by lead or its compounds can occur in several ways, including inhalation of the dusts or vapors, ingestion, or by direct absorption through the skin. In the case of the inorganic forms of lead, this last route is of no importance but it is of special importance in the case of the organic compounds of lead (11).

The toxic action of organolead compounds was recognized early in the commercial use of tetraethyllead as an antiknock compound. Trialkyllead derivatives have a dominant action on the central nervous system (1,2). A number of deaths occurred which dramatically pointed out this effect and led to an intensive evaluation of the toxic effects of tetraethyllead as well as of the methods

for its safe handling and use. Acute poisoning by lead antiknocks has been well documented, although relatively few cases have occurred in the United States since 1926 and virtually none since 1940. Sanders (12) stated in 1964 that 88 cases of tetraethyllead intoxication had occurred in the United States including 16 which terminated fatally, almost all of which occurred in connection with the cleaning of large tanks in which leaded gasoline had been stored. Fortunately, after recovery from the acute intoxication, the subsequent recovery has been complete without after effects (13).

The chelating agents, ethylenediaminetetraacetic acid (EDTA) and penicillamine are used in inorganic lead poisoning to increase the rate of excretion of lead, and chelation therapy has become generally accepted in this form of lead poisoning (14). EDTA has also been used in cases of poisoning by organolead antiknock compounds but with ambiguous results (15,16). The studies of Cremer *in vitro* (1,2) indicate that EDTA does not form a complex with the tetra- and tri-ethyllead compounds to any significant degree; this suggests that EDTA will have little effect on the rate of elimination of unmetabolized organolead compounds. It appears that penicillamine has not been used as a therapeutic agent to alleviate organic lead poisoning, but this ligand should be more effective than EDTA. The formation constant of the

trimethyllead-N-acetylpenicillamine complex is 4×10^5 ; this value is much greater than the formation constant (ca. 40) for binding of trimethyllead to the amino group of glycine which should be of similar magnitude to that for binding to one of the nitrogens of EDTA (17).

Considerable effort has been directed towards the elucidation of the mode of toxic action of organolead compounds. Activity of the two tetraalkylleads, tetramethyllead and tetraethyllead, is probably due to the trialkyllead ion produced by cleavage of one alkyl group from the tetraalkyllead. Compounds of the type R_3PbX are much more active physiologically than the other organolead types (1,2,18). Those compounds of the type R_4Pb and R_2PbX_2 which are physiologically active probably derive their activity from R_3PbX which is formed as they degrade in the body.

C. Coordination Chemistry of Trimethyllead.

The first coordination compounds of organolead, hydrates of diaryllead dinitrates and dicarboxylates, were reported in 1887 (19,20,21), but subsequent reports have been sparse. However a considerable amount of information is available on the chemistry of triorganotin(IV), including the trimethyltin(IV) species, and a small amount of information on the trimethylantimony(V) species. Most information is of a structural nature and

has been obtained from the use of vibrational spectroscopy and X-ray diffraction, but a small amount of information on the extent to which complexes form under equilibrium conditions has been obtained from potentiometric titrations. The coordination chemistry of trimethyltin(IV) and trimethylantimony(V) will be discussed in this section as it relates to that of trimethyllead(IV).

If possible, these trimethyl-metal species appear to favor a five-coordinate geometry. However, in situations where two additional ligands which form strong complexes with the trimethyl-metal species are not available, a tetrahedral (strictly, C_{3v} point group) structure is favoured. The trimethyllead halides in weakly-coordinating solvents such as benzene or chloroform provide an example of this situation (22). Drago and coworkers (23) have shown that such tetrahedral species are coordinately unsaturated by adding tetramethylenesulfoxide (TMSO) to carbon tetrachloride solutions of $(C_2H_5)_3PbCl$, $(CH_3)_3SnCl$ and $(C_2H_5)_3SnCl$. In each case, a 1:1 addition compound formed. The TMSO binds through an oxygen atom, and the formation constant for the lead complex, at 35°C, is 5.7 ± 0.8 . The ligands dimethylacetamide, dimethylformamide, and hexamethylphosphoramide behaved similarly. A trigonal bipyramidal structure, with the chloride and oxygen ligands occupying axial positions, was proposed on the basis of infrared and pmr measurements, and

confirmed by X-ray diffraction for the related adduct between trimethyltin chloride and pyridine (23). The coplanar nature of the metal atom and methyl groups is clearly shown in several crystal structures. The crystal structures of trimethyltin-fluoride (24) and -cyanide (25), and trimethyllead cyanide (25) are very similar and in each case planar trimethyl metal moieties are bridged by the anion. Infrared and Raman evidence suggest that this planarity is maintained in solution in both aqueous and coordinating organic solvents. There are many reports of the planar trimethyltin(IV) moiety in crystals which are based on the appearance in the infrared spectra of only one skeletal stretching band in the range 500 to 600 cm^{-1} (26). These are all compounds where the anion is a very hard base (26), and included are $(\text{CH}_3)_3\text{SnOH}$ (27,28), $(\text{CH}_3)_3\text{SnNO}_3$ (29) (but structure given as non-planar in ref. 30), $(\text{CH}_3)_3\text{SnClO}_4$ (30,31), $(\text{CH}_3)_3\text{SnBF}_4$ (32), $(\text{CH}_3)_3\text{SnAsF}_6$ (33), $(\text{CH}_3)_3^- \text{SbF}_6$ (33), $(\text{CH}_3)_3\text{Sn}(\text{HCOO})$ (34,35), the trimethyltin carboxylates (36,37) and trimethyltin compounds containing bifunctional nitrogen donors like imidazole (38,39,40). Raman spectroscopic measurements on aqueous solutions of the nitrate and perchlorate salts of the trimethyllead cation do not show evidence of lines attributable to vibration of Pb-O bonds involving water molecules in the first coordination sphere, but such vibrations are often

weak Raman scatterers. Three shifts attributable to Pb-C vibrations were observed (41,42), and the pattern (two relatively widely spaced shifts from stretching vibrations, and one from a deformation) is that expected for a planar PbC_3 skeleton. If the PbC_3 skeleton were markedly pyramidal, then a pattern consisting of four vibrations, two closely separated stretching modes and two deformation modes would be observed, as discussed by Downs and Steer (43). Raman spectroscopic studies of the aqueous solutions of the perchlorate and nitrate salts of $(\text{CH}_3)_3\text{Sn}^+$ (44) and $(\text{CH}_3)_3\text{Sb}^{2+}$ (43) have been interpreted similarly.

These observations are consistent with simple bonding theory. The trimethyl-metal ions in the absence of strong covalent bonding to the solvent or to the ligands would be expected to adopt a planar configuration to minimize the repulsions between the bonding pairs in the metal-carbon bonds or to maximize the S character in the metal orbitals used to bind the methyl groups (26). The additional favourable feature of this structure is that trans juxtaposition of the very soft CH_3^- ligands (45) is avoided.

Additional support for this structure in solution comes indirectly from measurement of the $^{207}\text{Pb}-^1\text{H}$ coupling constant. The metal-proton coupling constant is dependent on the amount of s character in the metal-carbon bond (46).

If the S, P_x , and P_y orbitals are responsible for binding in the plane and the P_z and d_{z^2} orbitals for binding at the axial positions of the bipyramidal structure, the coordination of different ligands in the axial position is not expected to cause a large change in the metal-proton coupling constant. However other effects besides the amount of S character in the metal-carbon bond may affect the coupling constant. For example, Shier and Drago (47) have shown that $J_{^{207}\text{Pb}-^1\text{H}}$ changes from 77.5 Hz for $(\text{CH}_3)_3\text{PbBF}_4$ in water to 85.0 Hz for $(\text{CH}_3)_3\text{PbClO}_4$ in hexamethylphosphoramide and that the change is not solely dependent upon any apparent geometrical change in the planar $(\text{CH}_3)_3\text{Pb}^+$ ion. Sayer reported (48) that $J_{^{207}\text{Pb}-^1\text{H}}$ changes from 77 Hz to 79 Hz upon formation of $(\text{CH}_3)_3\text{PbOH}$ from $(\text{CH}_3)_3\text{Pb}^+$ and from 77 Hz to 77.5 Hz upon formation of $(\text{CH}_3)_3\text{Pb}$ -carboxylate complexes from $(\text{CH}_3)_3\text{Pb}^+$. These results indicate that the $^{207}\text{Pb}-^1\text{H}$ coupling constant is not very sensitive to the complexation of trimethyllead. This implies that complex formation with the carboxylic acids studied does not bring about any significant change in the geometrical configuration of the Pb(IV) and the three methyl groups nor in the hybridization of the lead ion in trimethyllead (48,49).

From the X-ray crystal structure of trimethyllead cyanide and the Raman result for the trimethyllead cation in aqueous solution, and the more extensive results for

the related ion trimethyltin(IV), it seems probable that the aqueous trimethyllead cation has the trigonal bipyramidal structure with a water molecule in each of the axial positions. Complex formation will involve replacement of one or both water molecules by other ligands, and the previous studies suggest that complex formation will not have a major effect on the trigonal bipyramidal structure. An implication of this conclusion is that chelate formation is not favoured.

D. The Present Study.

In this thesis the results of a study of the aqueous solution chemistry of trimethyllead and of trimethyllead complexes of selected inorganic ligands are reported. The equilibrium constants for the acid-base equilibria of trimethyllead and the formation constants of the trimethyllead complexes of nine inorganic ligands were determined by proton nuclear magnetic resonance spectroscopy. This research was done as part of a larger effort directed toward characterizing the coordination chemistry of trimethyllead, and the role this might play in trimethyllead toxicology.

CHAPTER II
EXPERIMENTAL

A. Chemicals.

Sodium hydrogen sulfite, sodium sulfide and sodium iodide (J.T. Baker Chemicals), sodium thiosulfate, sodium chloride, and t-butanol (Fisher Scientific Company), sodium thiocyanate (Allied Chemicals), di-sodium hydrogen orthophosphate and sodium fluoride (British Drug Houses), sodium carbonate and sodium bromide (McArthur Chemicals) were used as received. In some cases, their solutions were standardized as described below. Sodium selenite (Alfa Inorganics) was purified before the solution was standardized. Trimethyllead acetate (Alfa Inorganics) was the only water soluble form of trimethyllead commercially available. Since the acetate ligand complexes trimethyllead in aqueous solution (48) and would thus interfere in these studies; the trimethyllead acetate was converted to a stock solution of trimethyllead perchlorate. Purification and standardization procedures are described below.

All other chemicals were of the highest grade commercially available and were used without further purification.

B. Preparation and Standardization of Trimethyllead(IV) Solutions.

Trimethyllead acetate was converted to a stock solution of trimethyllead perchlorate prior to use in the acid-base and complexation studies. An initial attempt by Dr. T. L. Sayer to extract $(CH_3)_3PbOH$ from benzene (48), using a method developed for triethyllead chloride (50), yielded only an insoluble, gelatinous mass of unknown composition. Ion exchange has been used to remove acetate from methylmercuric hydroxide solutions (51), and a similar method was developed for the conversion of trimethyllead acetate to trimethyllead perchlorate.

An approximately 0.25 M solution of trimethyllead acetate was filtered through a Nalgena filter unit of 0.2 μm pore size. The solution was then passed two or three times through an anion exchange column (Dowex 2 x 8) in the hydroxide form. The column was regenerated between passes with 1 M NaOH. The proton nuclear magnetic resonance (nmr) spectrum, at high amplitude, of an aliquot was then taken to confirm the absence of acetate (in acidic solution, the resonance of the methyl protons of acetate is located approximately 0.84 ppm downfield from the tert-butyl resonance of tertiary butanol and is detectable at concentration levels of ≥ 0.001 M). When no acetate could be detected, the solution was then

filtered again through a Nalgena filter unit of 0.2 μm pore size. The solution was then neutralized with concentrated perchloric acid (to pH ~5) and stored, tightly sealed, in the dark (50).

Before use, the stock solution of $(\text{CH}_3)_3\text{PbClO}_4$ was standardized by titration with NaOH using a glass electrode to locate the end point. The titrations were carried out using carbonate-free NaOH and the ionic strength was controlled using NaClO_4 . To ensure complete neutralization of all the $(\text{CH}_3)_3\text{PbOH}$ present in solution, the initial pH was reduced to a value ≈ 3 using concentrated HClO_4 . At this pH, the solution is a mixture of a strong acid (HClO_4) and a weak acid ($(\text{CH}_3)_3\text{Pb}^+$) and the titration yields two inflection points. Titration of the added perchloric acid gives a sharp inflection point at pH 5 and the $(\text{CH}_3)_3\text{Pb}^+$ an inflection point at pH 10.5. The exact position of the $(\text{CH}_3)_3\text{Pb}^+$ endpoint was determined using a second derivative plot of the titration curve (52). The titration with base converts the trimethyllead from $(\text{CH}_3)_3\text{Pb}^+$ to $(\text{CH}_3)_3\text{PbOH}$. Consequently, the amount of NaOH added between the first and second endpoints provides the concentration of trimethyllead in the stock solution.

The potentiometric method was verified by determining the trimethyllead concentration of several stock solutions using both atomic absorption spectroscopy, and EDTA

titration of aliquots following conversion to Pb^{2+} . The atomic absorption spectroscopy results tended to be slightly higher than the trimethyllead concentrations obtained by potentiometry, but the agreement is sufficient to support the potentiometric standardization. This method was used by Dr. T. L. Sayer and is fully described in his thesis (48). The EDTA titration method gave results which, within the standard deviation of the measurement, were identical with those from the potentiometric titrations (17). Since the EDTA method, which involves prolonged digestion of aliquots of the trimethyllead solution with aqua regia, is both time- and material-consuming, the potentiometric method of standardization has become the method routinely used in this laboratory.

C. Preparation and Standardization of Ligand Solutions.

A solution of sodium selenite, the source of the selenite ligand, was purified by first filtering off the insoluble materials. The sodium selenite then was isolated from water soluble impurities by recrystallization. Stock solutions of approximately 0.5 M sodium selenite in doubly-distilled water were prepared from the purified solid. Aliquots of the stock solutions were brought to low pH (~3) by adding $HClO_4$ and then were standardized by potentiometric titration with standard sodium hydroxide. At pH 3, the solution is a mixture

of strong acids and the weak acid HSeO_3^- ($\text{pK}_a \sim 7.83$).

The selenite concentration was determined from the volume of base between the two end points.

Disodium hydrogen orthophosphate was used as the source of the phosphate ligand. Stock solutions of approximately 0.1 M sodium phosphate in doubly-distilled water were prepared. Aliquots of the stock solutions were acidified and then were standardized by the procedure described above for solutions of sodium selenite.

Sodium hydrogen sulfite was used as the source of the sulfite ligand. The solid material was analyzed by oxidation of a known amount in aqueous solution with excess iodine followed by back-titration with standard thiosulfate, according to the equilibria represented by equation 4 and 5. The standard thiosulfate solution



was prepared by weighing the anhydrous reagent as a primary standard, and the resultant solution was used to standardize the iodine solution. Starch was used to locate the endpoint. A purity of 105.5% was obtained for the sodium hydrogen sulfite.

Sodium sulfide was used as the source of the sulfide ligand. The solid material was analyzed by dissolving a weighed amount, adding an excess of I_2 which oxidizes S^{2-} to $\text{S}_2\text{O}_3^{2-}$, and then back titration of the excess I_2 with $\text{S}_2\text{O}_3^{2-}$. A

purity of 90.0% was obtained for the sodium sulfide.

Standard solutions of base were prepared by dilution of saturated, carbonate-free sodium hydroxide with carbon dioxide-free distilled water. These solutions were standardized by titration against known amounts of primary standard potassium hydrogen phthalate.

D. pH Measurements.

pH measurements were carried out at $25 \pm 1^\circ\text{C}$ with an Orion Model 701 digital pH meter equipped with a standard glass electrode and a silver/silver chloride reference electrode in which sodium sulfate was used as the electrolyte solution. This reference electrode was used rather than the standard Ag/AgCl reference electrode with KCl electrolyte to avoid problems from the precipitation of KClO_4 in the reference electrode fiber junction. Fisher Certified standard solutions having pH values of 4.01, 7.00 and 10.00 at 25°C (potassium hydrogen phthalate, potassium phosphate, and sodium borate, respectively) were used to standardize the pH meter.

E. Proton Nuclear Magnetic Resonance Measurements.

Proton nuclear magnetic resonance (nmr) spectra were obtained on a Varian A-60-D high resolution spectrometer at a probe temperature of $25 \pm 1^\circ\text{C}$. The temperature of the probe was determined by measuring the potential

of a copper vs. constantan thermocouple inserted in the probe.

Spectra were recorded at sweep rates of 0.1 Hz/sec for the chemical shift measurements. Reported data are the average of at least three scans. Chemical shifts were measured relative to the tert-butyl resonance of internal tert-butanol but are reported relative to the methyl resonance of sodium 2,2-dimethyl-2-silapentane-5-sulfonic acid (DSS). Positive shifts correspond to resonances of protons less shielded than the methyl protons of DSS. The tert-butyl resonance of tert-butanol is 1.243 ppm downfield from the methyl resonance of DSS.

The sweep widths of the nmr recorder were calibrated by a sideband procedure. A Hewlett-Packard, Model 200 AB audio oscillator was used to provide sideband signals from TMS (12% in chloroform). The frequency of the sideband was counted with a Hewlett-Packard, Model 5307A High Resolution Counter. For recorder calibration, the shift of the sideband from the main signal, as indicated by the calibration markings of the recorder paper, was matched to the counted frequency generated by the audio oscillator.

F. Solutions for Nuclear Magnetic Resonance Measurements.

Solutions used in the nuclear magnetic resonance measurements were prepared in doubly distilled water

from pipetted amounts of stock trimethyllead perchlorate solution and weighed or pipetted amounts of the ligand. The concentration of trimethyllead in the solutions on which nmr measurements were made was 2.00×10^{-3} M or 5.00×10^{-3} M. Tert-butanol was added for an internal chemical shift reference at the same concentration as that of the trimethyllead. A background ionic strength of 0.3 M was maintained with NaClO_4 in all the experiments except those in the trimethyllead-thiocyanate study where an ionic strength of 1.5 M was used. In those experiments involving the measurement of chemical shift as a function of pH, the ionic strength of the solution was adjusted to 0.3 M and samples were withdrawn as the pH was varied. Variations in the ionic strength caused by changes in the chemical species in solution are small relative to the background ionic strength and also are minimized by the sampling method chosen. Initially, the solution was made alkaline to about pH 12.50. Then acid was added and samples were withdrawn at approximately 0.3 pH unit intervals until about pH 2. Typically, twenty five to thirty 0.4 ml samples were required to cover the pH range 2-12.5. Concentrated perchloric acid and sodium hydroxide solutions were used to adjust the pH. For example, a solution containing 5.00×10^{-3} M trimethyllead, 0.0500 M sodium sulfite and 0.113 M NaClO_4 was made alkaline with sodium hydroxide before samples

were withdrawn. Using the formation constant of trimethyl-lead sulfite calculated in Chapter IV and the K_a 's of the ligand, the concentration of each solution species, and thus the ionic strength of the solution, can be calculated at any pH. These calculations indicate that the ionic strength of this solution varied from 0.30 to 0.28 on going from pH 12.5 to pH 6.79, which is the pH region over which data was used for calculating the formation constants of the trimethyllead-sulfite complex. Similar calculations for other systems indicate the ionic strength variation to be small also. For example, for the trimethyl-lead-sodium selenite, the calculations indicate that the ionic strength varies from 0.30 at pH 12.5 to 0.28 at pH 7.83 to 0.27 at pH 2. The sulfite, selenite, and sulfide ligands are sensitive to air; therefore, solutions containing these anions were prepared with boiled and cooled water and in an argon atmosphere, using an appropriate amount of the crystalline salt of the ligand. Nmr spectra were obtained immediately after sample preparation.

For experiments involving chemical shift measurements as a function of pH, solutions of ligand to trimethyllead ratios varying from two to thirteen, as appropriate, were prepared.

Mole ratio experiments were performed at constant pH. Each sample required in these experiments was prepared individually; the required amounts of ligand and

trimethyllead were mixed, and sufficient solid sodium perchlorate was added to the solution to bring the ionic strength to 0.3 M (in the case of trimethyllead - sodium thiocyanate, the ionic strength was brought to 1.5 M). The pH was adjusted to the appropriate value with perchloric acid. The mole ratio experiments were at pH 4, and in one case 5, so that very little acid was required.

G. Determination of Formation Constants by NMR Spectroscopy.

The formation constants of the trimethyllead complexes were calculated from the chemical shift of the methyl protons of trimethyllead in solutions of known pH and known trimethyllead and ligand concentrations.

In this thesis, all the systems studied were found to be labile; that is, the trimethyllead moiety is exchanging between its various forms (aquated, hydroxy-complexed, and ligand-complexed) at a rate which is fast on the nmr time scale. Thus a single sharp resonance is observed for the methyl protons of trimethyllead and the observed chemical shift is the weighted average of the chemical shifts of the various trimethyllead species. That is,

$$\delta_{\text{obs}} = \sum_i p_i \delta_i \quad (6)$$

where δ_{obs} represents the observed, exchange-averaged

chemical shift of trimethyllead, and P_i is the fraction and δ_i is the chemical shift of the i th species in solution.

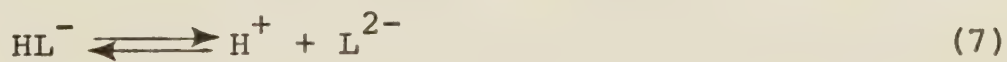
The formation constants and the chemical shifts of the complexes were determined from experiments where either the pH or the mole ratio was varied by curve-fitting the data to equation 6. The curve-fitting program used was generously supplied by Drs. J. L. Dye and V. A. Nicely of Michigan State University. This program, KINET, has been described in the literature (53). A user-supplied subroutine is required to describe the model to be fitted to the data. To use equation 6, it is necessary to solve for the various fractions, P_i . The fractions are calculated from the equations for the formation constants ($i-2$ such equations are defined for a binary system) and the mass balance equations for trimethyllead and ligand. Manipulation of the i equations to eliminate all but one fraction, P_x , gives a polynomial in P_x . The coefficients of P_x in this polynomial are in terms of the formation constants, the concentrations of hydrogen ion or hydroxide ion, the total trimethyllead and ligand concentration. Solution of this polynomial for P_x was achieved iteratively using the Library Subroutine DRTMI which is part of the SSP Library Subroutine Package; with this value for P_x , the other fractions were then calculated using the appropriate formation constant

equations. Once calculated, the fractions were then used to calculate a chemical shift with equation 6. The difference between this predicted chemical shift and the observed chemical shift was then reduced in the program KINET by systematically varying the initial guesses for the unknown formation constants and chemical shifts.

Examples of the application of the above procedure are described in detail in Chapter IV.

H. Determination of Acid Dissociation Constants of Selected Ligands by pH Titration.

The acid dissociation constants of some of the dibasic ligands were obtained by potentiometric titration using a glass electrode. The titrations were carried out using carbonate-free NaOH and the ionic strength was controlled at 0.3 M with NaClO_4 . The initial pH was reduced to a value of ~3 using concentrated HClO_4 . The solution is thus a mixture of strong acids, HClO_4 and $\text{H}_2\text{L}^{\text{L}}$, and a weak acid HL^- and the titration yields two inflection points. Titration of the strong acids yields a sharp inflection point at pH ~4-5 and that of HL^- yields a less sharp inflection point at higher pH. The acid dissociation constant, which is defined by equations 7 and 8, was determined from the pH titration data between



$$K_a = \frac{[H^+] [L^{2-}]}{[HL^-]} \quad (8)$$

the two inflection points.

CHAPTER III

TRIMETHYLLEAD SPECIES AND EQUILIBRIA IN AQUEOUS

SOLUTION

In this chapter, nmr results are reported for the aqueous solution chemistry of trimethyllead. The aqueous species have been identified and constants for the equilibria between the various species have been determined. This research was done in collaboration with Dr. T. L. Sayer, S. Backs, and Dr. C. A. Evans (49).

Results and Discussion

The proton magnetic resonance spectrum of trimethyllead in aqueous solution at approximately neutral pH is shown in Figure 1. The spectrum consists of a singlet flanked by two less intense satellite lines. The central resonance is assigned to the protons of methyl groups bonded to isotopes of lead having a nuclear spin of zero while the satellite resonances are due to protons of methyl groups bonded to ^{207}Pb , which has a nuclear spin of one-half (22.6% natural abundance). The chemical shift is given by the position of the central resonance and the lead-proton coupling constant by the separation of the satellite lines. Both the chemical shift of the methyl resonance and the lead-proton coupling constant are to some extent dependent on the nature of the ligand coordinated to the trimethyllead. To illustrate, the chemical shift of the

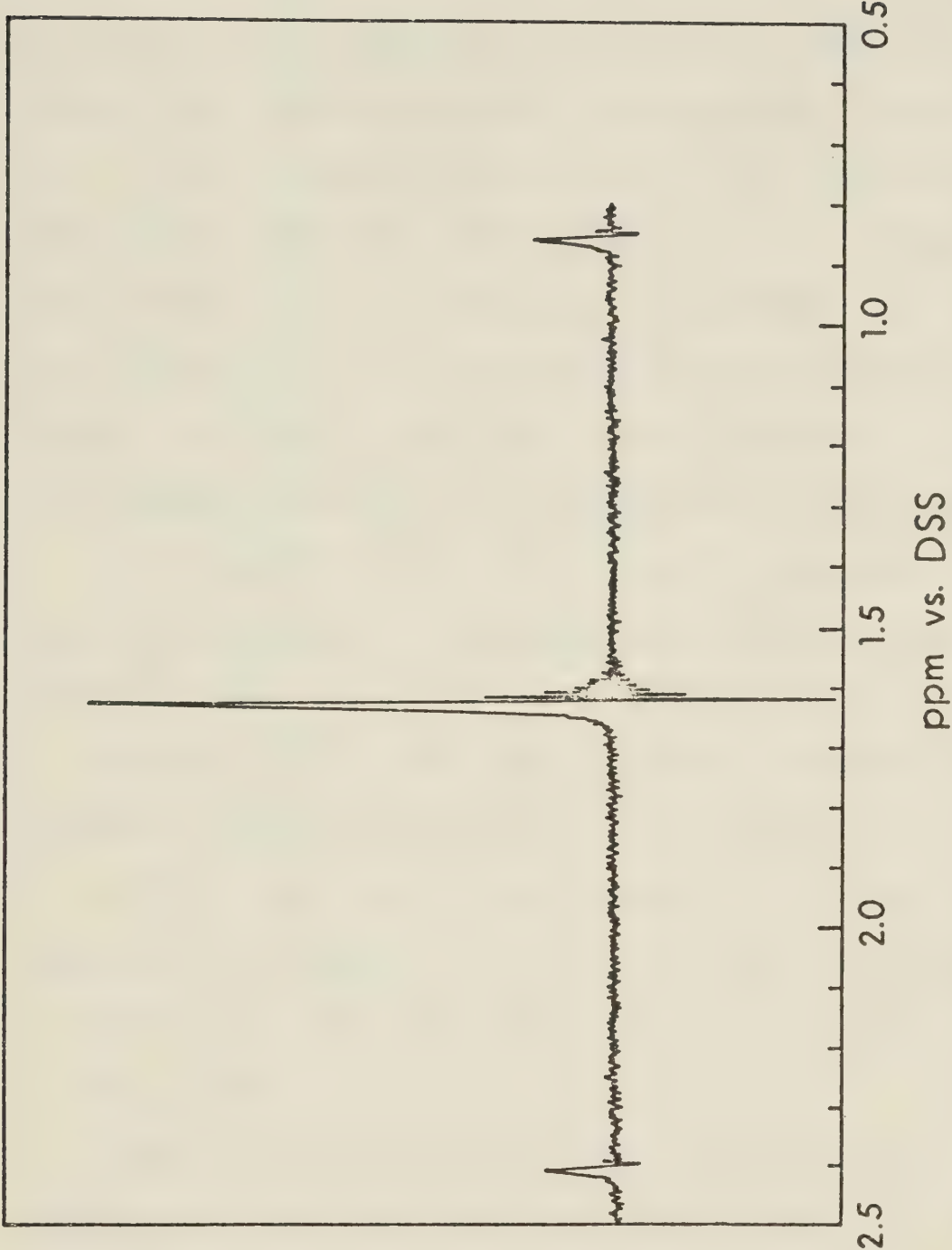
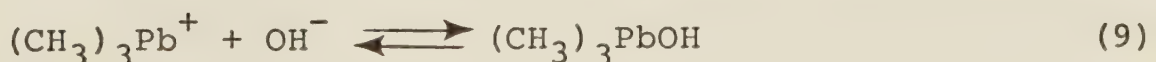


FIGURE 1. Proton NMR spectrum of the methyl groups of trimethyllead in 0.140 M solution at approximately neutral pH.

methyl resonance for a trimethyllead solution containing no coordinating ligand other than hydroxide ion is pH dependent. The chemical shift of the central resonance is shown as a function of pH in Figure 2 for a 5.00×10^{-3} M solution of trimethyllead perchlorate. Over this same pH range, the coupling constant varies from 77 Hz to 79 Hz (48). The pH dependence is due to the formation of trimethyllead hydroxide complexes as the pH is increased from acidic to basic. There is no evidence for the addition of more than one hydroxide ion per trimethyllead cation up to pH 12, at which point essentially all of the trimethyllead has been converted to $(\text{CH}_3)_3\text{PbOH}$.

The aqueous species of trimethyllead and the equilibrium constants for these species were determined from chemical shift vs. pH data of the type shown in Figure 2. Chemical shift data were used for solutions having trimethyllead concentrations in the range 5×10^{-3} M to 2×10^{-1} M. Representative chemical shift data are presented in Tables 1 and 2. At low pH, the trimethyllead is present as $(\text{CH}_3)_3\text{Pb}^+$, while at $\text{pH} > 12$ it is present as $(\text{CH}_3)_3\text{PbOH}$.

The first model tested involved a simple acid-base equilibrium for the conversion of $(\text{CH}_3)_3\text{Pb}^+$ to $(\text{CH}_3)_3\text{PbOH}$.



$$K_1 = \frac{[(\text{CH}_3)_3\text{PbOH}]}{[(\text{CH}_3)_3\text{Pb}^+] a_{\text{OH}^-}} \quad (10)$$

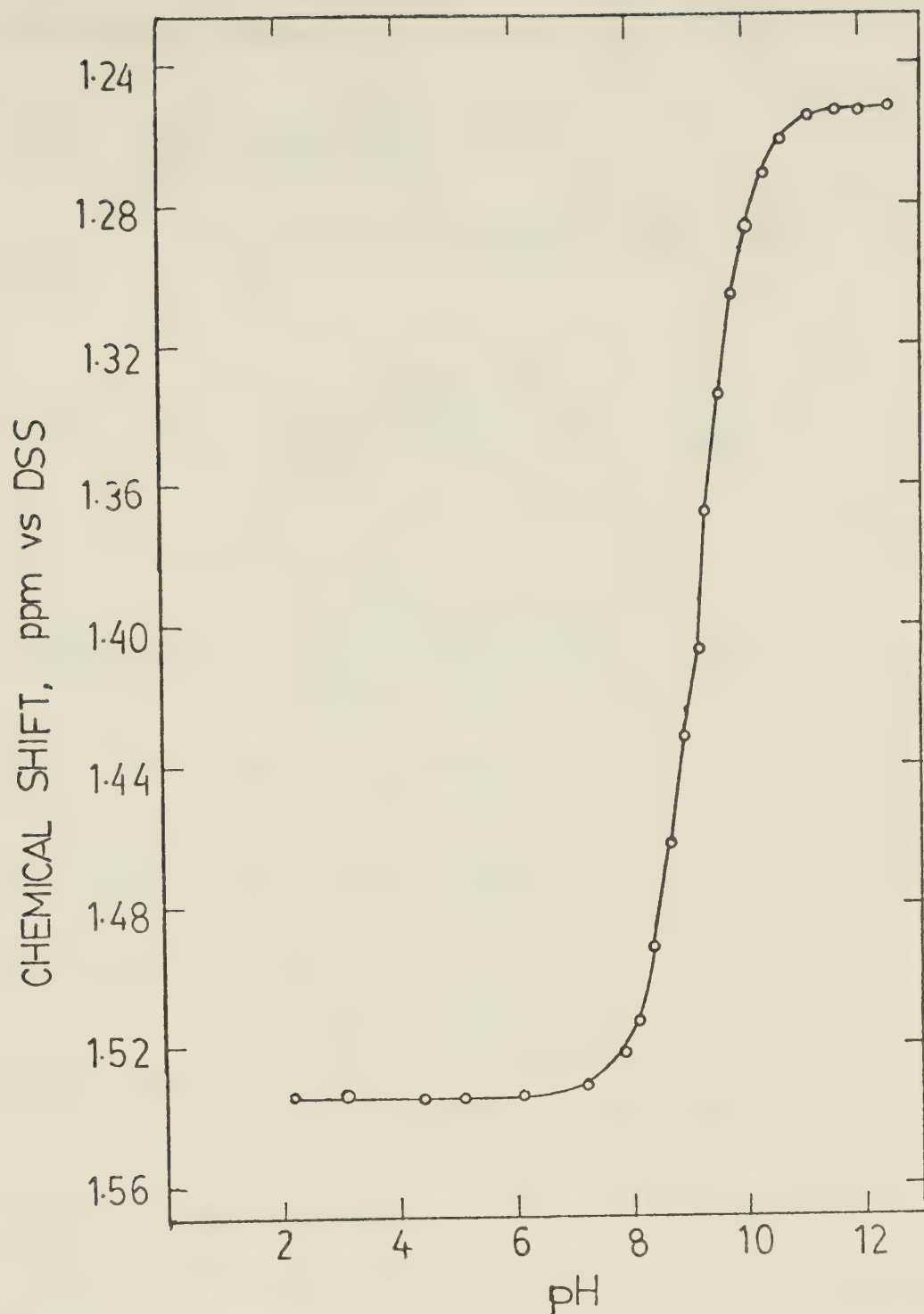


FIGURE 2. pH dependence of the chemical shift of the methyl protons of trimethyllead in an aqueous solution containing 5.00×10^{-3} M trimethyllead perchlorate.

For this model, Equation 6 becomes

$$\delta_{\text{obs}} = P_{(\text{CH}_3)_3\text{Pb}^+} + \delta_{(\text{CH}_3)_3\text{Pb}^+} + P_{(\text{CH}_3)_3\text{PbOH}} \delta_{(\text{CH}_3)_3\text{PbOH}} \quad (11)$$

where

$$P_{(\text{CH}_3)_3\text{Pb}^+} = \frac{[(\text{CH}_3)_3\text{Pb}^+]}{[(\text{CH}_3)_3\text{Pb}^+] + [(\text{CH}_3)_3\text{PbOH}]} \quad (12)$$

and

$$P_{(\text{CH}_3)_3\text{PbOH}} = \frac{[(\text{CH}_3)_3\text{PbOH}]}{[(\text{CH}_3)_3\text{Pb}^+] + [(\text{CH}_3)_3\text{PbOH}]} \quad (13)$$

Substitution of the relationship

$$1 = P_{(\text{CH}_3)_3\text{Pb}^+} + P_{(\text{CH}_3)_3\text{PbOH}} \quad (14)$$

into Equation 11 gives

$$P_{(\text{CH}_3)_3\text{PbOH}} = \frac{\delta_{\text{obs}} - \delta_{(\text{CH}_3)_3\text{Pb}^+}}{\delta_{(\text{CH}_3)_3\text{PbOH}} - \delta_{(\text{CH}_3)_3\text{Pb}^+}} \quad (15)$$

The observed chemical shift at low pH was taken as

$\delta_{(\text{CH}_3)_3\text{Pb}^+}$ (1.535 ppm) and that at pH > 12 as $\delta_{(\text{CH}_3)_3\text{PbOH}}$ (1.253 ppm). In the intermediate pH region where δ_{obs} is between these two values, $P_{(\text{CH}_3)_3\text{PbOH}}$ was calculated directly from δ_{obs} with Equation 15. From this value and Equations 12-14, $[(\text{CH}_3)_3\text{PbOH}]$ and $[(\text{CH}_3)_3\text{Pb}^+]$ were obtained, from which K_1 was calculated. This procedure was repeated at each δ_{obs} intermediate between $\delta_{(\text{CH}_3)_3\text{Pb}^+}$ and $\delta_{(\text{CH}_3)_3\text{PbOH}}$.

In Table 1 are presented the results obtained for a 5.00×10^{-3} M solution of trimethyllead. The $\log K_1$ is seen to be relatively constant over the pH range 7.18 to 10.67, with variations of a random rather than systematic

TABLE 1

Chemical Shift Data and Calculated Values for $\log K_1$ for Trimethyllead.^{a,b}

pH	$\delta_{\text{observed}}^c$	$\log K_1^b$
2.18	1.534	
3.10	1.534	
4.42	1.535	
5.08	1.535	
6.11	1.534	
7.18	1.531	4.96
7.83	1.522	4.83
8.13	1.514	4.78
8.39	1.492	4.86
8.69	1.462	4.85
8.92	1.431	4.84
9.18	1.390	4.84
9.34	1.368	4.82
9.59	1.335	4.79
9.81	1.306	4.82
10.09	1.287	4.77
10.37	1.272	4.77
10.67	1.262	4.82
11.16	1.255	
11.59	1.253	
11.99	1.253	
12.54	1.252	

FOOTNOTES for TABLE 1

- a) 5.00×10^{-3} M trimethyllead perchlorate.
- b) 25°C; Ionic strength 0.30 M (NaClO_4).
- c) ppm vs DSS.

nature. The average is $\log K_1 = 4.83 \pm 0.05$, where the uncertainty is the standard deviation.

In Table 2, the results obtained for a 0.185 M solution of trimethyllead are presented. Examination of the results indicates that at this higher concentration there is a continuous decrease in $\log K_1$ as the pH increases. This indicates that the model represented by Equations 9 and 10 does not completely describe the aqueous solution chemistry at this higher concentration. The concentration dependence, evident by comparison of the results in Table 1 with those in Table 2, suggests that at the higher concentration additional species form from $(\text{CH}_3)_3\text{Pb}^+$ and $(\text{CH}_3)_3\text{PbOH}$ by unsymmetrical equilibria. Because of the unsymmetrical nature of the equilibria, the position of equilibrium will favour the simple species $(\text{CH}_3)_3\text{Pb}^+$ and $(\text{CH}_3)_3\text{PbOH}$ at the lower concentration.

TABLE 2

Chemical Shift Data and Calculated Values for $\log K_1$ for
Trimethyllead.^{a,b}

pH	$\delta_{\text{observed}}^c$	$\log K_1^b$
1.91	1.535	
3.78	1.535	
5.22	1.534	
6.12	1.530	6.09
7.08	1.515	5.80
7.41	1.496	5.79
7.77	1.481	5.60
7.98	1.464	5.54
8.23	1.443	5.45
8.48	1.423	5.33
8.74	1.400	5.22
9.05	1.377	5.05
9.27	1.359	4.95
9.49	1.340	4.85
9.77	1.318	4.75
10.04	1.302	4.64
10.28	1.286	4.59
10.60	1.273	4.51
10.81	1.266	4.48
11.04	1.262	4.46
11.31	1.257	4.49
11.57	1.256	
11.94	1.254	
12.26	1.252	
12.57	1.252	
12.78	1.253	

a) 0.185 M trimethyllead perchlorate.

b) 25°C; Ionic strength 0.30 M (NaClO_4).

c) ppm vs DSS.

Of the various models tested, the best fit to the nmr chemical shift titration data was obtained with the model described by Equations 9, 10, 16 and 17.



$$K_2 = \frac{[((\text{CH}_3)_3\text{Pb})_2\text{OH}^+]}{[(\text{CH}_3)_3\text{Pb}^+] [(\text{CH}_3)_3\text{PbOH}]} \quad (17)$$

where K_1 and K_2 are the formation constants for mononuclear and dinuclear hydroxide complexes, respectively, and a_{OH^-} is the hydroxide ion activity. $((\text{CH}_3)_3\text{Pb})_2\text{OH}^+$ can be considered to form by association of $(\text{CH}_3)_3\text{Pb}^+$ and $(\text{CH}_3)_3\text{PbOH}$ as represented by Equation 16. As the total trimethyl-lead concentration decreases, the position of this equilibrium will shift to the left in favour of $(\text{CH}_3)_3\text{Pb}^+$ and $(\text{CH}_3)_3\text{PbOH}$. For the model described by Equations 9, 10, 16 and 17, Equation 6 becomes

$$\begin{aligned} \delta_{\text{obs}} = & P_{(\text{CH}_3)_3\text{Pb}^+} \delta_{(\text{CH}_3)_3\text{Pb}^+} + P_{(\text{CH}_3)_3\text{PbOH}} \delta_{(\text{CH}_3)_3\text{PbOH}} \\ & + P_{((\text{CH}_3)_3\text{Pb})_2\text{OH}^+} \delta_{((\text{CH}_3)_3\text{Pb})_2\text{OH}^+} \end{aligned} \quad (18)$$

where

$$P_{(\text{CH}_3)_3\text{Pb}^+} = \frac{[(\text{CH}_3)_3\text{Pb}^+]}{[(\text{CH}_3)_3\text{Pb}^+] + [(\text{CH}_3)_3\text{PbOH}] + 2[((\text{CH}_3)_3\text{Pb})_2\text{OH}^+]} \quad (19)$$

$$P_{(\text{CH}_3)_3\text{PbOH}} = \frac{[(\text{CH}_3)_3\text{PbOH}]}{[(\text{CH}_3)_3\text{Pb}^+] + [(\text{CH}_3)_3\text{PbOH}] + 2[((\text{CH}_3)_3\text{Pb})_2\text{OH}^+]} \quad (20)$$

$$P_{((CH_3)_3Pb)_2OH^+} = \frac{2[((CH_3)_3Pb)_2OH^+]}{[(CH_3)_3Pb^+] + [(CH_3)_3PbOH] + 2[((CH_3)_3Pb)_2OH^+]} \quad (21)$$

Rearrangement of Equation 10 to Equation 22,

$$[(CH_3)_3PbOH] = K_1 a_{OH^-} [(CH_3)_3Pb^+] \quad (22)$$

and dividing both sides of this equation by the total trimethyllead concentration yields Equation 23.

$$P_{(CH_3)_3PbOH} = K_1 a_{OH^-} P_{(CH_3)_3Pb^+} \quad (23)$$

In the same way, $P_{((CH_3)_3Pb)_2OH^+}$ can be expressed in terms of K_1 , K_2 , a_{OH^-} and $P_{(CH_3)_3Pb^+}$. Substitution of these relationships for $P_{(CH_3)_3PbOH}$ and $P_{((CH_3)_3Pb)_2OH^+}$ into Equation 18 gives Equation 24

$$\begin{aligned} \delta_{obs} &= P_{(CH_3)_3Pb^+} \delta_{(CH_3)_3Pb^+} + K_1 a_{OH^-} P_{(CH_3)_3Pb^+} \delta_{(CH_3)_3PbOH} \\ &\quad + 2K_1 K_2 a_{OH^-} P_{(CH_3)_3Pb^+}^2 \delta_{((CH_3)_3Pb)_2OH^+} \end{aligned} \quad (24)$$

$P_{(CH_3)_3Pb^+}$ is then expressed in terms of K_1 , K_2 and the total trimethyllead concentration as follows. The mass balance for trimethyllead is

$$\begin{aligned} [(CH_3)_3Pb]_{total} &= [(CH_3)_3Pb^+] + [(CH_3)_3PbOH] \\ &\quad + 2[((CH_3)_3Pb)_2OH^+] \end{aligned} \quad (25)$$

$[(CH_3)_3Pb]_{total}$ represents the total concentration of

trimethyllead. Dividing both sides of the equation by $[(\text{CH}_3)_3\text{Pb}]_{\text{total}}$ leads to Equation 26.

$$1 = P_{(\text{CH}_3)_3\text{Pb}^+} + P_{(\text{CH}_3)_3\text{PbOH}} + P_{((\text{CH}_3)_3\text{Pb})_2\text{OH}^+} \quad (26)$$

Substitution of K_1 , a_{OH^-} and $P_{(\text{CH}_3)_3\text{Pb}^+}$ for $(\text{CH}_3)_3\text{PbOH}$ and the analogous relationship for $P_{((\text{CH}_3)_3\text{Pb})_2\text{OH}^+}$ into Equation 26 leads to

$$\begin{aligned} 1 &= P_{(\text{CH}_3)_3\text{Pb}^+} + K_1 a_{\text{OH}^-} P_{(\text{CH}_3)_3\text{Pb}^+} \\ &\quad + 2K_1 K_2 a_{\text{OH}^-} P_{(\text{CH}_3)_3\text{Pb}^+}^2 \end{aligned} \quad (27)$$

Solution of this equation for $P_{(\text{CH}_3)_3\text{Pb}^+}$ by the quadratic formula gives

$$P_{(\text{CH}_3)_3\text{Pb}^+} = \frac{(- (1 + K_1 a_{\text{OH}^-}) + ((1 + K_1 a_{\text{OH}^-})^2 + 8K_1 K_2 a_{\text{OH}^-} \cdot [(\text{CH}_3)_3\text{Pb}]_{\text{total}})^{\frac{1}{2}})}{4K_1 K_2 a_{\text{OH}^-} \cdot [(\text{CH}_3)_3\text{Pb}]_{\text{total}}} \quad (28)$$

K_1 , K_2 and $\delta_{((\text{CH}_3)_3\text{Pb})_2\text{OH}^+}$ were evaluated from chemical shift data, over the pH range 0.5-13.0 and trimethyllead concentrations in the range $5 \times 10^{-3}\text{M}$ to $2 \times 10^{-1}\text{ M}$, using the non-linear least squares curve fitting program KINET (53). The chemical shifts of the cationic $(\text{CH}_3)_3\text{Pb}^+$ and neutral $(\text{CH}_3)_3\text{PbOH}$ were taken as the limiting shifts of sufficiently acidic and alkaline solutions, respectively. The curve fitting procedure involved using Equation 24 and 28. These were supplied as a subroutine to the curve fitting program KINET. The program was then given initial estimates for K_1 , K_2 and

δ_{pred} of $((\text{CH}_3)_3\text{Pb})_2\text{OH}^+$. It then calculates $P_{((\text{CH}_3)_3\text{Pb})_2\text{OH}^+}$ with Equation 28 followed by δ_{pred} with Equation 24 at pH and $[(\text{CH}_3)_3\text{Pb}]_{\text{total}}$ values corresponding to the experimental data using the estimates for K_1 , K_2 and δ_{pred} of $((\text{CH}_3)_3\text{Pb})_2\text{OH}^+$. The non-linear least squares program then compares δ_{obs} to δ_{pred} , and adjusts K_1 , K_2 and δ_{pred} of $((\text{CH}_3)_3\text{Pb})_2\text{OH}^+$ to minimize the sum of the squares of the residuals (SSR) (defined by Equation 29).

$$\text{SSR} = \sum_i (\delta_{i,\text{pred}} - \delta_{i,\text{obs}})^2 \quad (29)$$

By this procedure, the values $K_1 = 7.34 (\pm 0.1) \times 10^4 \text{ M}^{-1}$ and $K_2 = 3.12 (\pm 0.1) \times 10^1 \text{ M}^{-1}$ were obtained for the formation constants of trimethyllead hydroxide and the trimethyllead dimer, where the uncertainties are linear estimates of the standard deviation. The chemical shifts of the species are 1.535 ($(\text{CH}_3)_3\text{Pb}^+$), 1.253 ($(\text{CH}_3)_3\text{PbOH}$), and 1.327 ppm ($((\text{CH}_3)_3\text{Pb})_2\text{OH}^+$), quoted from DSS.

Because of the unsymmetrical nature of the equilibrium for the formation of $((\text{CH}_3)_3\text{Pb})_2\text{OH}^+$ (Equation 16), the extent to which $((\text{CH}_3)_3\text{Pb})_2\text{OH}^+$ forms is dependent on the total concentration of trimethyllead and the pH; reducing the total concentration of trimethyllead present in solution reduces the concentration of $((\text{CH}_3)_3\text{Pb})_2\text{OH}^+$. To illustrate, the species distribution, calculated using the above values of K_1 and K_2 and a trimethyllead concentration of 0.200 M, is shown in Figure 3. Figure 4 shows

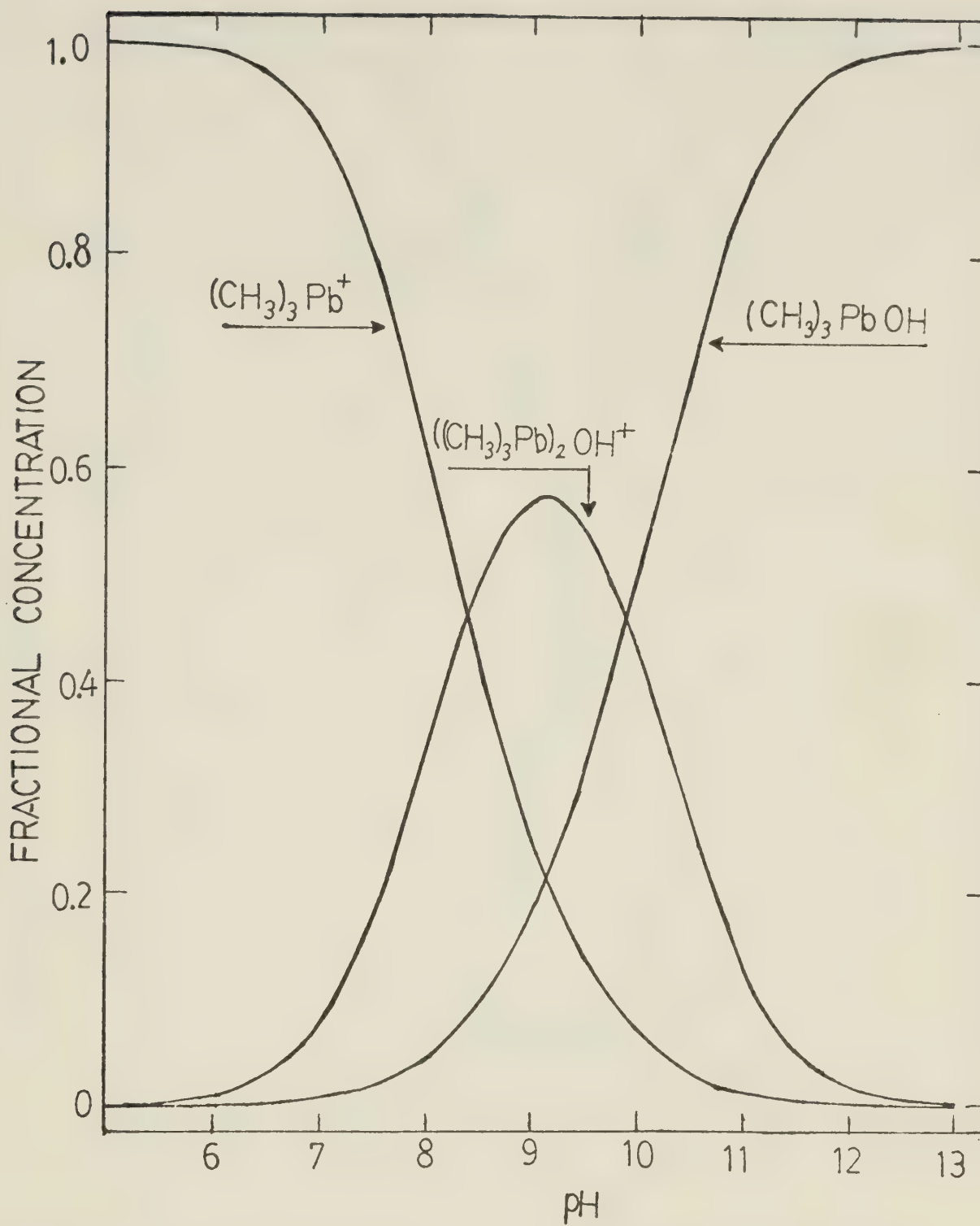


FIGURE 3. pH dependence of the trimethyllead species distribution in a 0.200 M aqueous solution calculated using K_1 and K_2 as in the text.

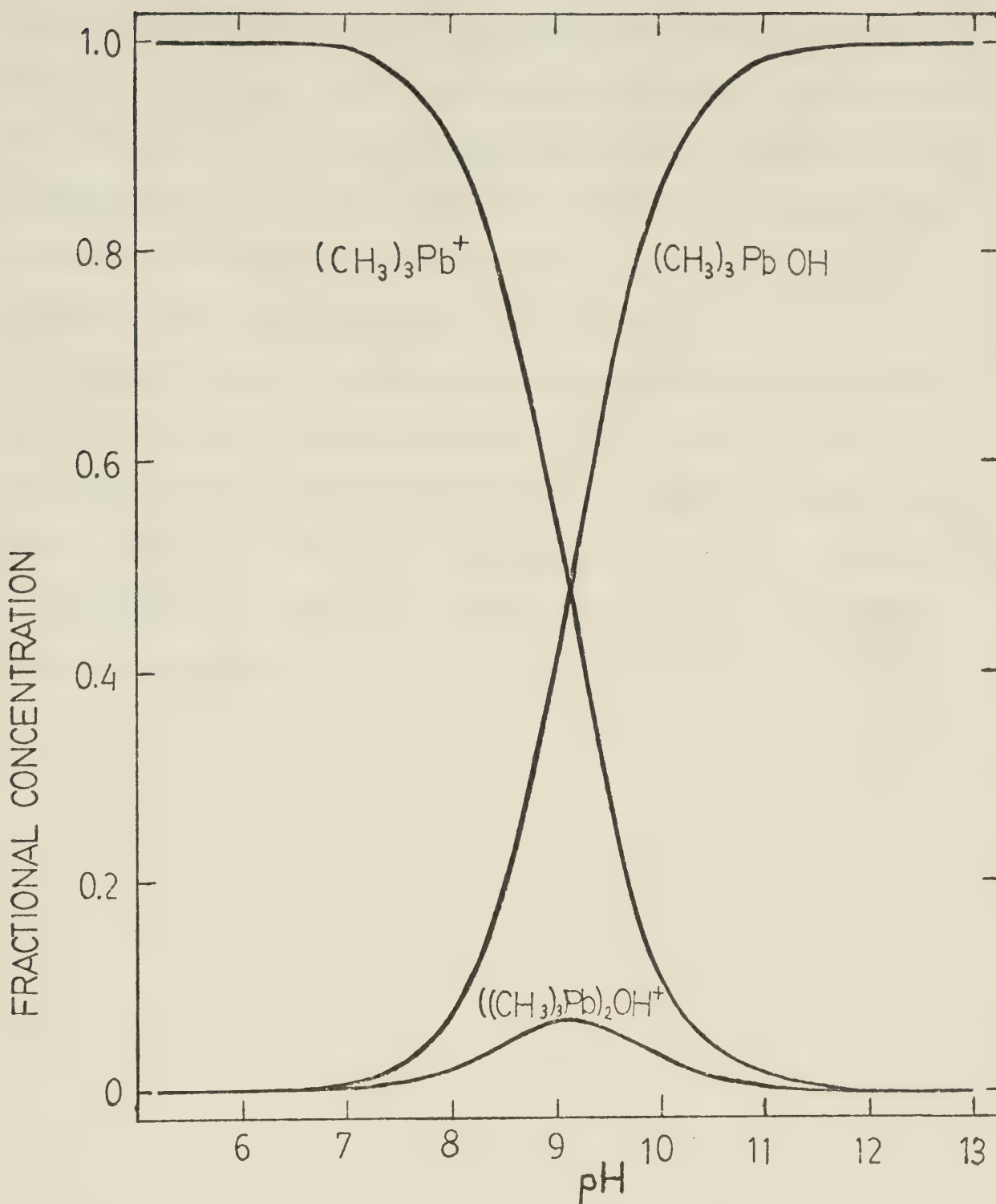


FIGURE 4. pH dependence of the trimethyllead species distribution in a 5.00×10^{-3} M aqueous solution calculated using K_1 and K_2 as in the text.

species distribution at a trimethyllead concentration of 5.00×10^{-3} M. At a total trimethyllead concentration of 5.00×10^{-3} M, the maximum fractional concentration of trimethyllead as $((\text{CH}_3)_3\text{Pb})_2\text{OH}^+$ is 0.07 as compared to a maximum fractional concentration of 0.57 at a total trimethyllead concentration of 0.200 M.

There are no reports in the literature of studies of the aqueous solution chemistry of trimethyllead for comparison with the results of this study. However, the model which best fits the experimental data is analogous to that for the aqueous solution equilibria of methyl-mercury (51,54,55).

CHAPTER IV

TRIMETHYLLLEAD COMPLEXES OF SELECTED INORGANIC ANIONS

The results of a study of the complexation of trimethyllead by the inorganic anions sulfite, selenite, thiosulfate, thiocyanate, sulfide, phosphate, carbonate, iodide, bromide, chloride, and fluoride are presented in this chapter. The complexation of these ligands by trimethyllead was studied by nmr, using the chemical shift titration method.

A. Results

1. The Sulfite and Selenite Complexes of Trimethyllead.

The binding of trimethyllead by the sulfite and selenite ligands, SO_3^{2-} and SeO_3^{2-} , was investigated by monitoring the chemical shift of the methyl protons of trimethyllead as a function of solution conditions. Solutions having ligand-to-trimethyllead ratios of 12:1 for the sulfite system and 10:1 for the selenite system were used in these studies to maximize the fraction of trimethyllead complexed. Because of the easy oxidation of sulfite by dissolved oxygen, solutions were prepared with boiled and cooled water and in an argon atmosphere, using an appropriate amount of the crystalline salt of the ligand. Spectra were obtained immediately after sample preparation.

The chemical shift of the methyl protons of trimethyllead is presented as a function of pH in Figure 5 for both a solution of trimethyllead perchlorate (open points) and a solution containing trimethyllead perchlorate and sodium hydrogen sulfite (solid points). Similar data are shown in Figure 6 for the trimethyllead-selenite system.

The two chemical shift titration curves in Figure 5 are different over the pH range 4.5-11, indicating some complexation of trimethyllead by sulfite over this pH range. At high pH, hydroxide ion competes with the sulfite for the trimethyllead, while at low pH protons compete with the trimethyllead for the sulfite (pK_2 of $H_2SO_3 = 6.79$). Similarly, the data in Figure 6 indicate some complexation of trimethyllead by selenite over the pH range 5-12.

Formation constants were calculated for trimethyllead-sulfite and trimethyllead-selenite complexes from the chemical shift data in Figures 5 and 6. The procedure will be discussed in detail, using the trimethyllead-sulfite system as an example.

Because the exchange of trimethyllead between its various forms in trimethyllead-sulfite solutions is fast on the nmr time scale, separate nmr signals are not observed for the complexed species. Rather, an averaged resonance is obtained. To determine the formation

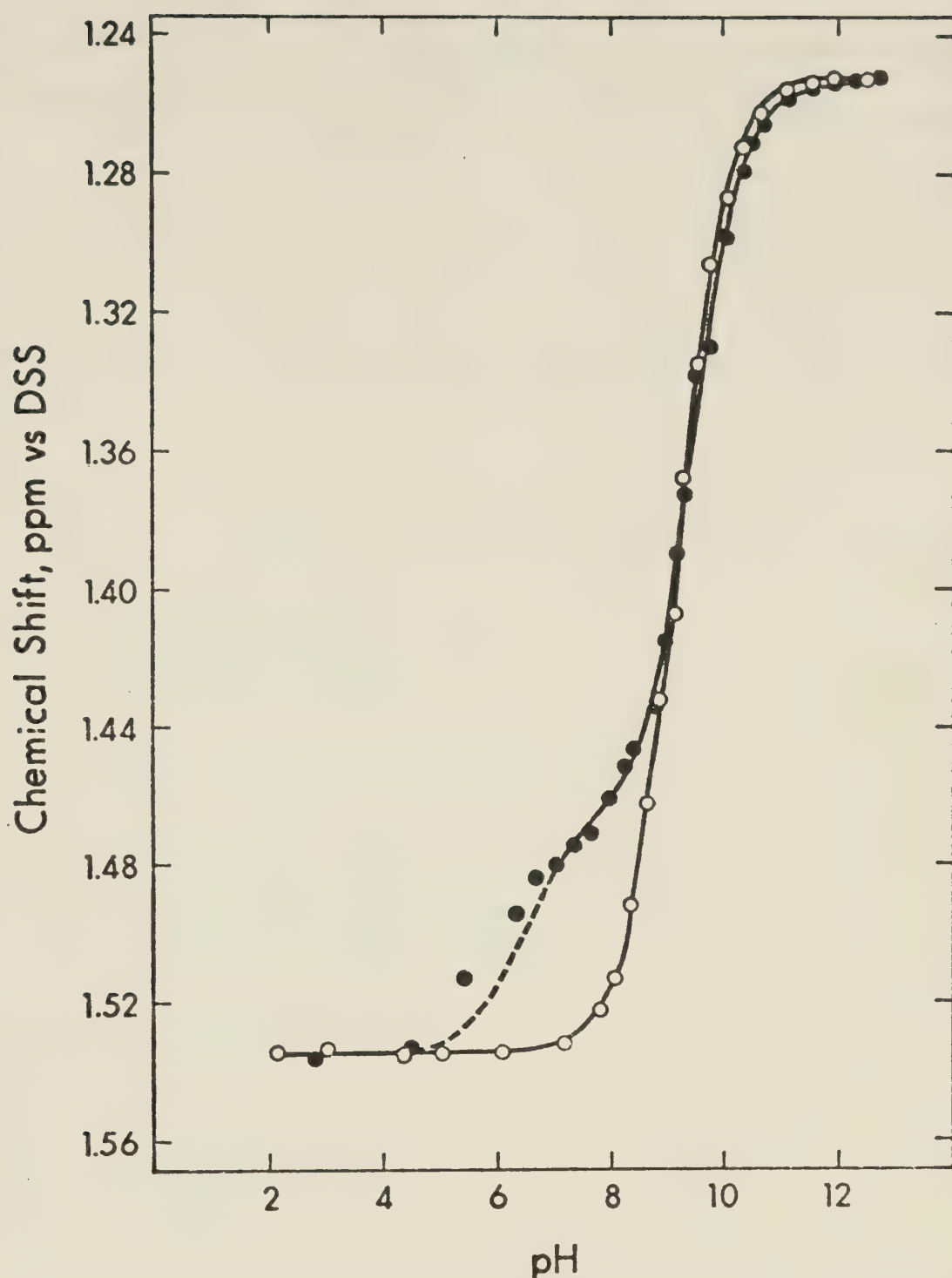
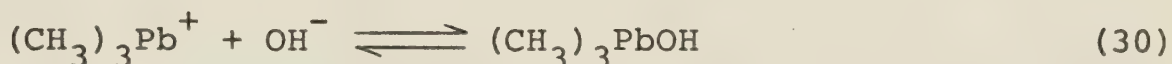


FIGURE 5. pH dependence of the chemical shift of the methyl protons of trimethyllead in an aqueous solution containing 5.00×10^{-3} M trimethyllead perchlorate (open points) and in an aqueous solution containing 5.00×10^{-3} M trimethyllead perchlorate and 0.0612 M sodium hydrogen sulfite (solid points).

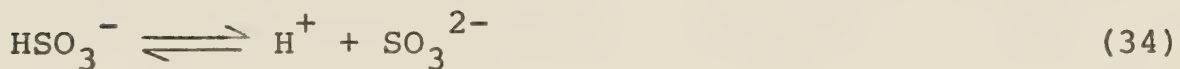
constants from the averaged chemical shift, models must be proposed for the complexation equilibria. The experimental data is then fit to the models. Of the various models tested, the best fit was obtained for a model in which the trimethyllead and sulfite form a simple one-to-one complex. The equations which describe this model are:



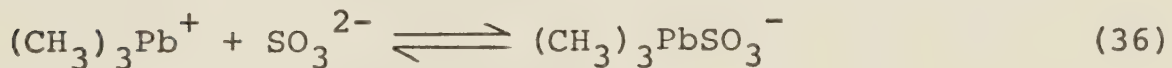
$$K_1 = \frac{[(CH_3)_3PbOH]}{[(CH_3)_3Pb^+]a_{OH^-}} \quad (31)$$



$$K_2 = \frac{[((CH_3)_3Pb)_2OH^+]}{[(CH_3)_3Pb^+] [(CH_3)_3PbOH]} \quad (33)$$



$$K_a = \frac{a_{H^+} [SO_3^{2-}]}{[HSO_3^-]} \quad (35)$$



$$k_f = \frac{[(CH_3)_3PbSO_3^-]}{[(CH_3)_3Pb^+] [SO_3^{2-}]} \quad (37)$$

where $K_1 = 7.34 (\pm 0.1) \times 10^4$ and $K_2 = 3.12 (\pm 0.1) \times 10^1$ (Chapter III), and a_{OH^-} and a_{H^+} represent the activity

of hydroxide ion and that of hydrogen ion, respectively.

K_a is the acid dissociation constant of HSO_3^- which was determined to be 1.62×10^{-7} by pH titration with standard NaOH. K_f is the formation constant of the trimethyllead-sulfite complex. For the model defined by Equations 30-37, the exchange-averaged chemical shift is described by Equation 38.

$$\begin{aligned} \delta_{\text{obs}} = & P_{(\text{CH}_3)_3\text{Pb}^+} \delta_{(\text{CH}_3)_3\text{Pb}^+} + P_{(\text{CH}_3)_3\text{PbOH}} \delta_{(\text{CH}_3)_3\text{PbOH}} \\ & + P_{((\text{CH}_3)_3\text{Pb})_2\text{OH}^+} \delta_{((\text{CH}_3)_3\text{Pb})_2\text{OH}^+} \\ & + P_{(\text{CH}_3)_3\text{PbSO}_3^-} \delta_{(\text{CH}_3)_3\text{PbSO}_3^-} \end{aligned} \quad (38)$$

where P refers to the fraction of the total trimethyllead in that form and δ to its chemical shift. The values used for $\delta_{(\text{CH}_3)_3\text{Pb}^+}$, $\delta_{(\text{CH}_3)_3\text{PbOH}}$ and $\delta_{((\text{CH}_3)_3\text{Pb})_2\text{OH}^+}$ were obtained from the study described in Chapter III. The fractions are defined by Equations 39-42.

$$P_{(\text{CH}_3)_3\text{Pb}^+} = \frac{[(\text{CH}_3)_3\text{Pb}^+]}{[(\text{CH}_3)_3\text{Pb}]_{\text{total}}} \quad (39)$$

$$P_{(\text{CH}_3)_3\text{PbOH}} = \frac{[(\text{CH}_3)_3\text{PbOH}]}{[(\text{CH}_3)_3\text{Pb}]_{\text{total}}} \quad (40)$$

$$P_{((\text{CH}_3)_3\text{Pb})_2\text{OH}^+} = \frac{[((\text{CH}_3)_3\text{Pb})_2\text{OH}^+]}{[(\text{CH}_3)_3\text{Pb}]_{\text{total}}} \quad (41)$$

$$P_{(CH_3)_3PbSO_3^-} = \frac{[(CH_3)_3PbSO_3^-]}{[(CH_3)_3Pb]_{\text{total}}} \quad (42)$$

$$\text{where } [(CH_3)_3Pb]_{\text{total}} = [(CH_3)_3Pb^+] + [(CH_3)_3PbOH] + 2[(CH_3)_3Pb)_2OH^+] + [(CH_3)_3PbSO_3^-] \quad (43)$$

The formation constant was evaluated from the chemical shift data by fitting the data to Equation 38 with the nonlinear least squares program KINET. The curve fitting procedure involves:

- (a) Estimating initial values for K_f and $\delta_{(CH_3)_3PbSO_3^-}$.
- (b) With this estimate for K_f , the computer program then calculates $P_{(CH_3)_3Pb^+}$, $P_{(CH_3)_3PbOH}$, $P_{((CH_3)_3Pb)_2OH^+}$, and $P_{(CH_3)_3PbSO_3^-}$ at the pH of a given data point (by the procedure described below).
- (c) With these fractional concentrations, the estimate for $\delta_{(CH_3)_3PbSO_3^-}$ and the known values for the other chemical shifts, the program then predicts a value for the exchange-averaged chemical shift ($\delta_{i,\text{pred}}$) at that pH.
- (d) Steps (b) and (c) are then repeated for each data point in the data set.
- (e) The program then compares the predicted chemical shifts to the observed chemical shifts by calculating the sum of the squares of the residuals (SSR).
- (f) The program then adjusts K_f and $\delta_{(CH_3)_3PbSO_3^-}$ to minimize the SSR.

(g) Steps (b) through (f) are then repeated until the best values for K_f and $\delta_{(CH_3)_3PbSO_3^-}$ are obtained from the particular experimental data, as indicated by the minimum in the SSR.

Steps (c)-(f) are performed by the program KINET. The user supplies a model equation (Equation 38 in this application) by means of a subroutine. The calculations in step (b) are performed with user supplied equations in the same subroutine.

The procedure in step (b) for the calculation of the populations will now be described. The procedure involved first calculating the concentration of $(CH_3)_3Pb^+$, by using the mass balance expression for the trimethyl-lead (Equation 43) and that for the ligand (Equation 44).

$$[SO_3^{2-}]_{\text{total}} = [HSO_3^-] + [SO_3^{2-}] + [(CH_3)_3PbSO_3^-] \quad (44)$$

By substitution of Equations 31, 33, 35, and 37 into Equations 43 and 44, Equations 45 and 46 are obtained.

$$\begin{aligned} [(CH_3)_3Pb]_{\text{total}} &= [(CH_3)_3Pb^+] (1 + K_1 a_{OH^-} \\ &\quad + 2K_1 K_2 a_{OH^-} [(CH_3)_3Pb^+] \\ &\quad + \frac{K_a K_f}{a_{H^+}} [HSO_3^-]) \end{aligned} \quad (45)$$

$$[SO_3^{2-}]_{\text{total}} = [HSO_3^-] (1 + \frac{K_a}{a_{H^+}} + \frac{K_a K_f}{a_{H^+}} [(CH_3)_3Pb^+]) \quad (46)$$

Rearrangement of Equation 46 leads to

$$[\text{HSO}_3^-] = \frac{[\text{SO}_3^{2-}]_{\text{total}}}{1 + \frac{K_a}{a_{\text{H}^+}} + \frac{K_a K_f}{a_{\text{H}^+}} [(\text{CH}_3)_3\text{Pb}^+]} \quad (47)$$

Substitution of Equation 47 into Equation 45 and rearranging yields a polynomial equation in $[(\text{CH}_3)_3\text{Pb}^+]$.

$$\begin{aligned} & \frac{2K_1 K_2 K_a K_f a_{\text{OH}^-}}{a_{\text{H}^+}} [(\text{CH}_3)_3\text{Pb}^+]^3 + \left(\frac{(1+K_1 a_{\text{OH}^-}) K_a K_f}{a_{\text{H}^+}} \right. \\ & \left. + 2K_1 K_2 a_{\text{OH}^-} \left(1 + \frac{K_a}{a_{\text{H}^+}} \right) \right) [(\text{CH}_3)_3\text{Pb}^+]^2 \\ & + \left((1 + K_1 a_{\text{OH}^-}) \left(1 + \frac{K_a}{a_{\text{H}^+}} \right) + \frac{K_a K_f}{a_{\text{H}^+}} ([\text{SO}_3^{2-}]_{\text{total}} \right. \\ & \left. - [(\text{CH}_3)_3\text{Pb}]_{\text{total}}) \right) [(\text{CH}_3)_3\text{Pb}^+] \\ & - [(\text{CH}_3)_3\text{Pb}]_{\text{total}} \left(1 + \frac{K_a}{a_{\text{H}^+}} \right) = 0 \end{aligned} \quad (48)$$

The coefficients in this polynomial are functions of K_1 , K_2 , K_a , $[(\text{CH}_3)_3\text{Pb}]_{\text{total}}$, and $[\text{SO}_3^{2-}]_{\text{total}}$ (which are known), a_{H^+} and a_{OH^-} (which are known experimental parameters) and K_f (which is estimated initially and the estimate is then refined by the nonlinear least squares program). The first step in the calculation of $[(\text{CH}_3)_3\text{Pb}^+]$

was to calculate each of the coefficients, and then to solve the polynomial with the subroutine DRTMI, which is part of the SSP Library Subroutine Package. $[(\text{CH}_3)_3\text{PbOH}]$ was then calculated by substitution of this value for $[(\text{CH}_3)_3\text{Pb}^+]$ into Equation 31 and $[((\text{CH}_3)_3\text{Pb})_2\text{OH}^+]$ by substitution of these two concentrations into Equation 33. $[\text{HSO}_3^-]$ was calculated by substitution of the value for $[(\text{CH}_3)_3\text{Pb}^+]$ into Equation 47, and from this value $[\text{SO}_3^{2-}]$ was calculated with Equation 35. $[(\text{CH}_3)_3\text{PbSO}_3^-]$ was then calculated by substitution of this value and $[(\text{CH}_3)_3\text{Pb}^+]$ into Equation 37. The populations were then calculated by substitution of these concentrations into Equations 39-42.

The K_f obtained for the $(\text{CH}_3)_3\text{PbSO}_3^-$ complex by this procedure using data covering the pH range 7 to 12.7 is 18.8 ± 1 , where the uncertainty is a linear estimate of the standard deviation (provided by the computer program KINET). A value of 1.407 ppm was obtained simultaneously for $\delta(\text{CH}_3)_3\text{PbSO}_3^-$. Attempts to fit chemical shift data covering the pH range 3 to 7 to this model were unsuccessful, with large differences between the observed and predicted chemical shifts. In this pH region, the free sulfite is predominantly in the form HSO_3^- , suggesting that the species $(\text{CH}_3)_3\text{PbHSO}_3$ might also be forming at pH less than 7. Attempts to fit the observed chemical shift data to a model involving

the species $(\text{CH}_3)_3\text{PbHSO}_3$ in addition to the four species in the model described above resulted in a formation constant for which the linear estimate of the standard deviation was considerably larger than the formation constant. This suggests that the concentration of $(\text{CH}_3)_3\text{PbHSO}_3$ must be small, or that some other complex is present. Consequently, the model represented by Equations 30-37 describes the trimethyllead-sulfite system only at pH greater than 7. The observed and predicted chemical shifts for this pH region are in good agreement (Figure 5). The difference between the predicted chemical shift curve (dashed curve at pH < 7 in Figure 5) and the experimental points indicates that other trimethyllead-sulfite complexes must be forming in this pH range. Selenium and sulfur are both Group VI elements, and their coordination chemistry is similar. The behavior of selenite anions towards trimethyllead is expected to be similar to that of sulfite. The similarity of the nmr titration curves for trimethyllead-selenite solutions to those of trimethyllead-sulfite solutions indicates this to be the case. The two chemical shift titration curves in Figure 6 are different over the pH range 5-12, indicating some complexation of trimethyllead by selenite over this pH range. The titration curves show that selenite competes more strongly with hydroxide for the trimethyllead than does sulfite

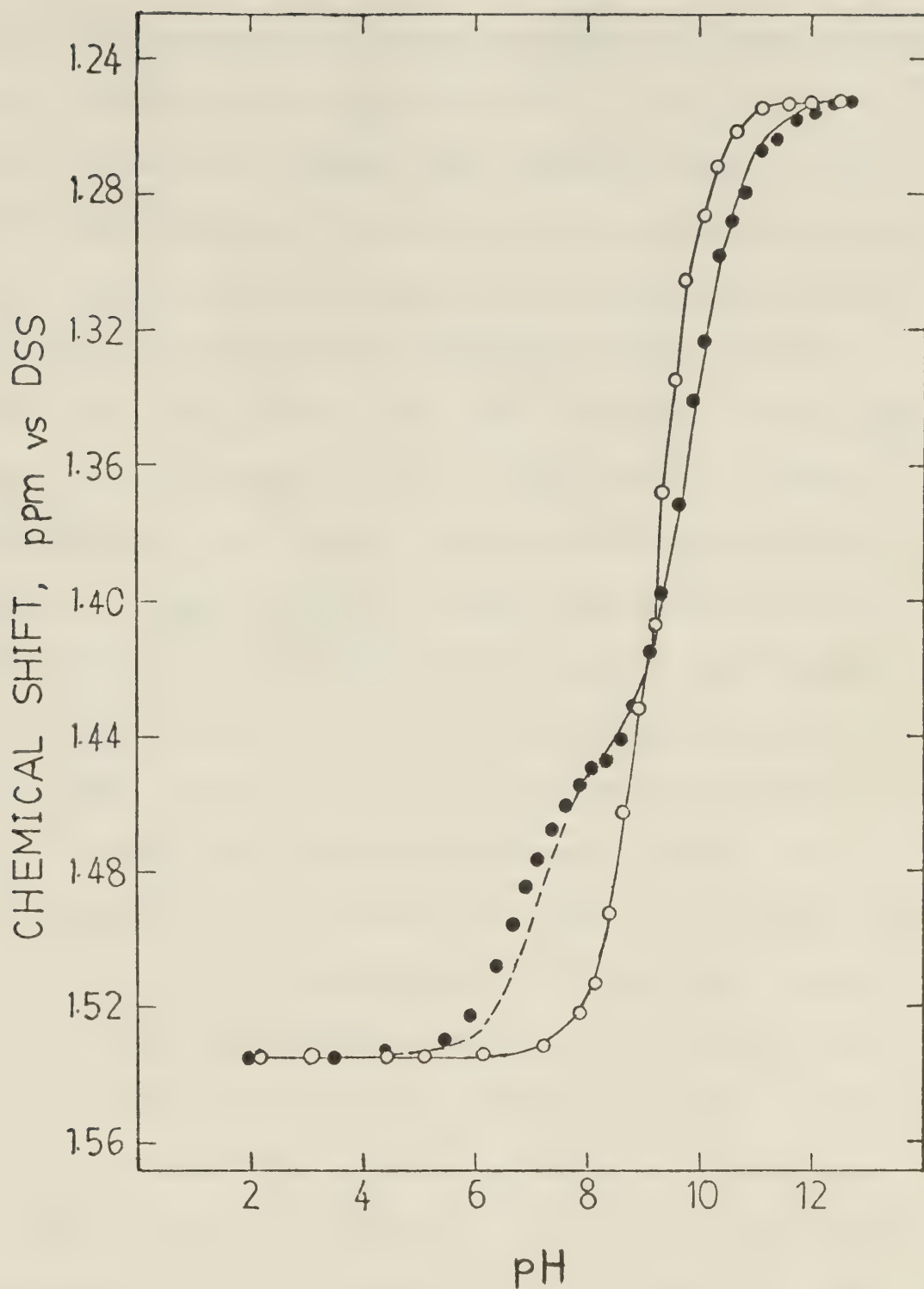


FIGURE 6. pH dependence of the chemical shift of the methyl protons of trimethyllead in an aqueous solution containing 5.00×10^{-3} M trimethyllead perchlorate (open points) and in an aqueous solution containing 4.83×10^{-3} M trimethyllead perchlorate and 0.0504 M sodium selenite (solid points).

at high pH. At low pH protons compete with the trimethyllead for the selenite (pK_2 of $H_2SeO_3 = 7.83$).

The formation constant and chemical shift of the trimethyllead-selenite complex were determined from the chemical shift versus pH data by the method described above for the trimethyllead-sulfite complex. The K_f obtained for $(CH_3)_3PbSeO_3^-$ by this procedure using data covering the pH range 7.8 to 12.7 is 90.4 ± 4 , where the uncertainty is a linear estimate of the standard deviation. $\delta_{(CH_3)_3PbSeO_3^-} = 1.425$ ppm was obtained simultaneously. Attempts to fit chemical shift data covering the pH range 2 to 7.8 to this model were unsuccessful, as was the case in the trimethyllead-sulfite system, with large differences between the observed and predicted chemical shifts. In this pH region, the free selenite is predominantly in the form $HSeO_3^-$, suggesting that the species $(CH_3)_3PbHSeO_3$ might also be forming at pH less than 7.8. Attempts to fit the observed chemical shift data to a model involving the species $(CH_3)_3PbHSeO_3$ were unsuccessful, which suggests that the concentration of $(CH_3)_3PbHSeO_3$ must be small, or that some other complex is present. Consequently, the model represented by Equations 30-37 describes the trimethyllead-selenite system only at pH greater than 7.8. The observed and predicted chemical shifts for this pH region are in good agreement (Figure 6). The difference between

the predicted chemical shift curve (dashed curve at pH < 7.8 in Figure 6) and the experimental points indicates that other trimethyllead-selenite complexes must be forming in this pH range.

There are no formation constants for trimethyllead-sulfite or trimethyllead-selenite complexes available for comparison with the results obtained in this study. However, it is of interest to compare them with the formation constants for the analogous methylmercury complexes of these ligands (Table 3). These results indicate that the trimethyllead-sulfite and -selenite complexes are both weak compared with the methylmercury complexes of these ligands. Also, the formation constant of the trimethyllead-selenite complex is larger than that of the sulfite complex, the opposite of the order found for the formation constants of the methylmercury complexes. In the methylmercury complexes, methylmercury binds to sulfur in $\text{CH}_3\text{Hg}(\text{SO}_3)^-$ and to oxygen in $\text{CH}_3\text{Hg}(\text{SeO}_3)^-$.

2. The Thiosulfate Complex of Trimethyllead

The binding of trimethyllead by the thiosulfate ligand, $\text{S}_2\text{O}_3^{2-}$, was investigated by monitoring the chemical shift of the methyl protons of trimethyllead in solutions containing trimethyllead and thiosulfate as a function of solution conditions. Solutions having thiosulfate-to-trimethyllead ratios of 10:1 were used in this study to maximize the fraction of trimethyllead complexed. The

TABLE 3

Summary of Acid Dissociation Constants and Formation
 Constants of the Trimethyllead and Methylmercury Complexes
 of Selected Inorganic Ligands, and the Trimethyllead
 Chemical Shifts of Their Trimethyllead Complexes.

Ligand	pK_a^a	$\delta_{\text{complex}}^b$	K_f^a $(\text{CH}_3)_3\text{PbX}$	$\log K_f^c$ CH_3HgX
SO_3^{2-}	6.79	1.407	18.8	7.96
SeO_3^{2-}	7.83	1.425	90.4	6.46
$\text{S}_2\text{O}_3^{2-}$		1.504	138	11.05
SCN^-		1.709	0.381 ^d	6.05
HPO_4^{2-}	6.71	1.435	75.1	
CO_3^{2-}	10.30	1.347	396	6.10
I^-		1.867	1.89	8.60
Br^-		1.692	1.95	6.62
Cl^-		1.595	1.22	5.25

a) 25°C; Ionic strength 0.3 M (NaClO_4) unless otherwise noted.

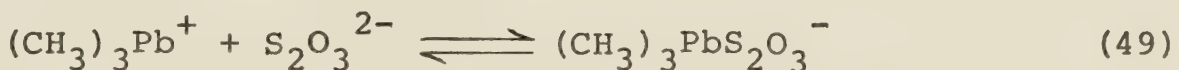
b) ppm vs DSS.

c) References 51 and 56.

d) 1.5 M ionic strength (NaClO_4).

chemical shift of the methyl protons of trimethyllead is presented as a function of pH in Figure 7 for both a solution of trimethyllead perchlorate (open points) and a solution containing trimethyllead perchlorate and sodium thiosulfate (solid points).

The two chemical shift titration curves in Figure 7 are different over the pH range 2-12.5, indicating some complexation of trimethyllead by thiosulfate over this pH range. At high pH, hydroxide ion competes with the thiosulfate for the trimethyllead. At low pH, trimethyllead is present as trimethyllead-thiosulfate and the free, aqueous forms of trimethyllead. At pH < 2.8, a precipitate formed, presumably from the decomposition of $S_2O_3^{2-}$. Of the various models tested, the best fit was obtained for a model in which the trimethyllead and thiosulfate form a simple one-to-one complex, $(CH_3)_3Pb(S_2O_3)^-$.



$$K_f = \frac{[(CH_3)_3PbS_2O_3^-]}{[(CH_3)_3Pb^+][S_2O_3^{2-}]} \quad (50)$$

The formation constant and chemical shift of the trimethyllead-thiosulfate complex were determined from the chemical shift versus pH data by the method described above for the trimethyllead-sulfite complex. The K_f obtained for $(CH_3)_3PbS_2O_3^-$ by this procedure using data

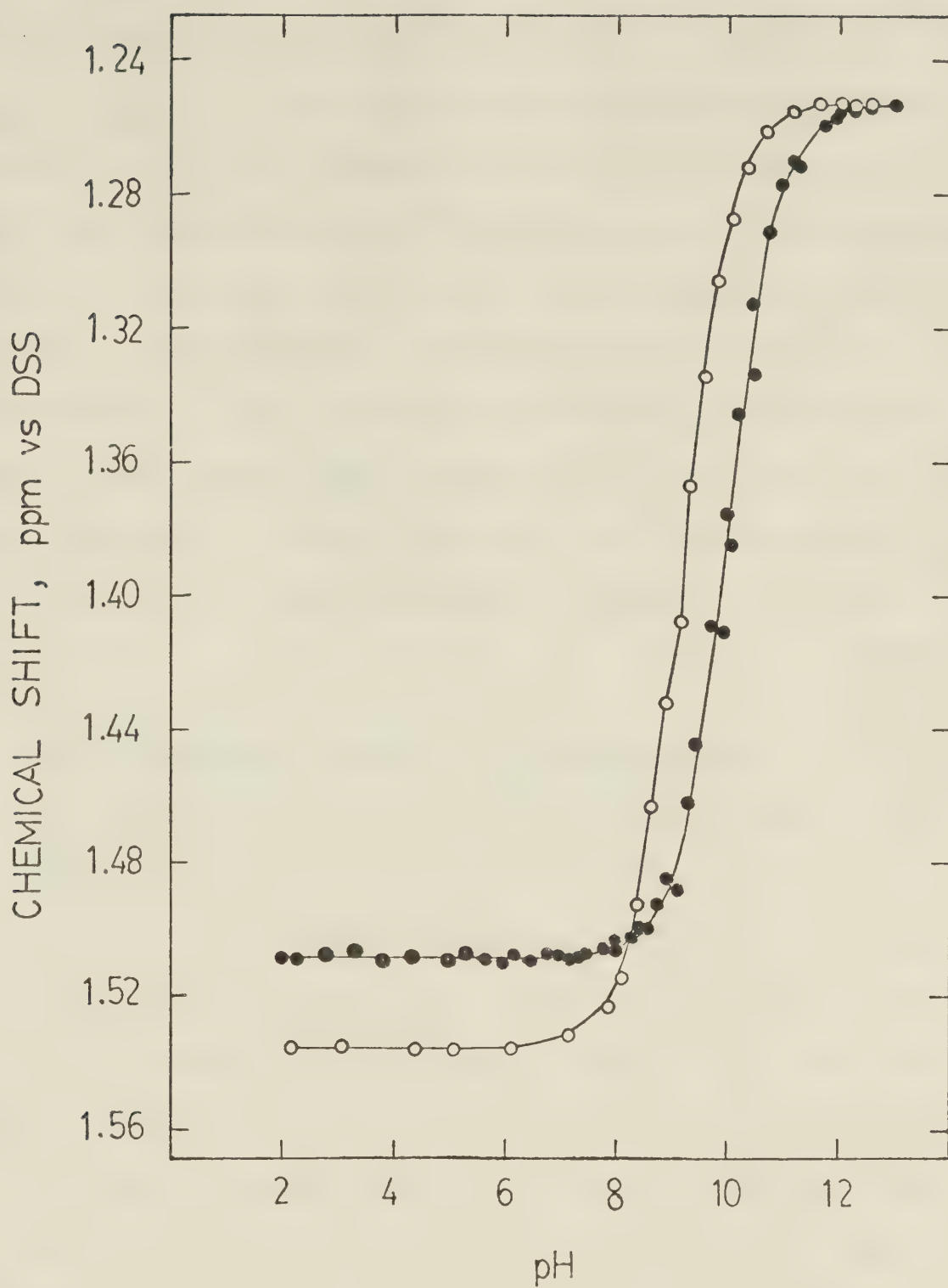


FIGURE 7. pH dependence of the chemical shift of the methyl protons of trimethyllead in an aqueous solution containing 5.00×10^{-3} M trimethyllead perchlorate (open points) and in an aqueous solution containing 5.00×10^{-3} M trimethyllead perchlorate and 0.0503 M sodium thiosulfate (solid points).

covering the pH range 2 to 13 is 138 ± 3 (Table 3).

$\delta_{\text{Pb}}^{(\text{CH}_3)_3\text{PbS}_2\text{O}_3^-} = 1.504$ ppm was obtained simultaneously.

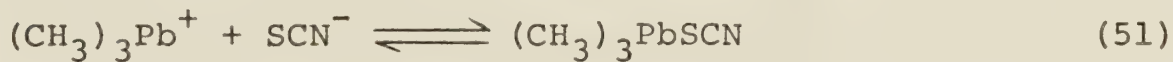
Attempts to fit the observed chemical shift data to a model involving the species $(\text{CH}_3)_3\text{Pb}(\text{S}_2\text{O}_3)_2^{3-}$ in addition to the four species in the model described above gave poor fits. Consequently, the model represented by Equations 30-33 and 49,50 describes the trimethyllead-thiosulfate system. The observed and predicted chemical shifts for the pH region where all the sample points were taken are in good agreement (Figure 7) with this model.

3. The Thiocyanate Complex of Trimethyllead

The formation constant and the chemical shift of the trimethyllead-thiocyanate complex were determined by monitoring the chemical shift of the methyl protons of trimethyllead in solutions containing different mole ratios of trimethyllead and thiocyanate. At first, the chemical shift of the trimethyllead in solutions containing the same concentrations of ligand and trimethyllead was measured as a function of pH. The chemical shift titration curves for solutions containing thiocyanate are quite similar to those containing no thiocyanate over the entire pH region, indicating that thiocyanate interacts only weakly with trimethyllead. In order to maximize the fraction of trimethyllead in the complexed form, this system was studied by mole ratio experiments

at a constant pH, which was chosen so as to minimize competition from the hydroxide ions for the trimethyllead. 14 samples whose ratios of sodium thiocyanate to trimethyllead ranged from 0 to 300 were prepared individually at pH 5. The chemical shift of the methyl protons of trimethyllead is presented as a function of the $[\text{NaSCN}]_{\text{total}} / [(\text{CH}_3)_3\text{Pb}]_{\text{total}}$ ratio in Figure 8. The ionic strength was kept constant at 1.5 M with NaClO_4 . A higher ionic strength was used for this system because of the wider range of mole ratios necessary to obtain the formation constant. The results in Figure 8 indicate that the observed chemical shift varies as the ligand to trimethyllead ratio is changed, providing evidence that SCN^- forms a complex with trimethyllead.

The chemical shift changes continuously over the range of ligand-to-trimethyllead ratios in Figure 8, so that it is not possible to obtain the chemical shift of the complex directly. The formation constant was calculated for the trimethyllead-thiocyanate complex from the chemical shift data by fitting the data to a model. In the model which gives the best fit, the trimethyllead and thiocyanate form a simple one-to-one complex. The equations which describe this model are 51 and 52.



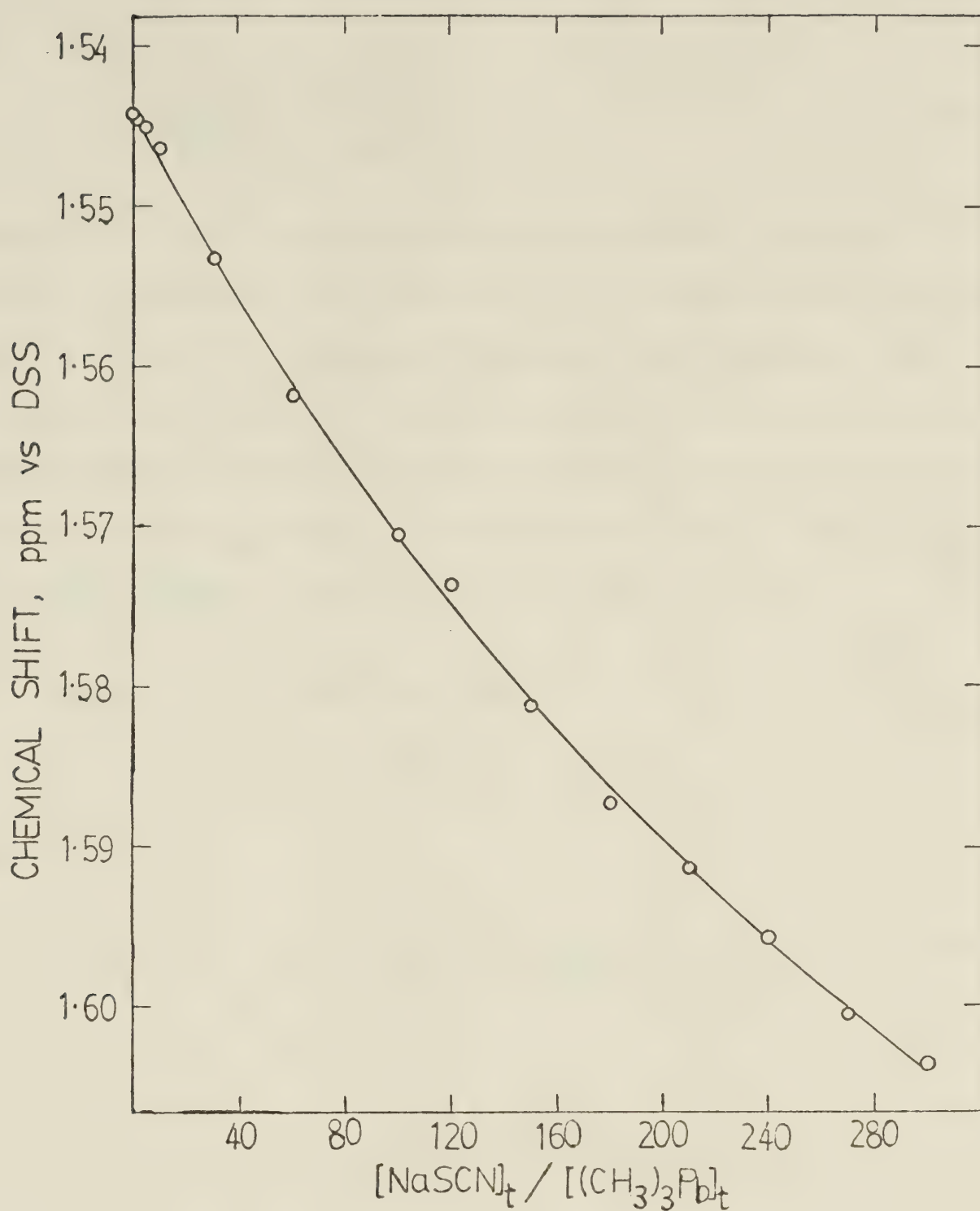


FIGURE 8. Mole ratio dependence of the chemical shift of the methyl protons of trimethyllead in aqueous solutions having sodium thiocyanate and trimethyllead perchlorate ratios between 0-300 at pH 5.00. Trimethyllead perchlorate = 5.00×10^{-3} M, Ionic strength = 1.5 M (NaClO₄ as required).

$$K_f = \frac{[(\text{CH}_3)_3\text{PbSCN}]}{[(\text{CH}_3)_3\text{Pb}^+][\text{SCN}^-]} \quad (52)$$

Exchange of the trimethyllead moiety between the two species in solution was observed to be rapid on the nmr time scale and thus the formation constant and chemical shift of the complex were determined by similar but much simpler procedures to those outlined previously for the trimethyl-lead-sulfite equilibria. For the above model, the exchange-averaged chemical shift is described by

$$\begin{aligned} \delta_{\text{obs}} = & P(\text{CH}_3)_3\text{Pb}^+ + \delta(\text{CH}_3)_3\text{Pb}^+ \\ & + P(\text{CH}_3)_3\text{PbSCN} + \delta(\text{CH}_3)_3\text{PbSCN} \end{aligned} \quad (53)$$

where

$$P(\text{CH}_3)_3\text{Pb}^+ = \frac{[(\text{CH}_3)_3\text{Pb}^+]}{[(\text{CH}_3)_3\text{Pb}^+] + [(\text{CH}_3)_3\text{PbSCN}]} \quad (54)$$

and

$$P(\text{CH}_3)_3\text{PbSCN} = \frac{[(\text{CH}_3)_3\text{PbSCN}]}{[(\text{CH}_3)_3\text{Pb}^+] + [(\text{CH}_3)_3\text{PbSCN}]} \quad (55)$$

Rearrangement of Equation 52 and substitution into Equation 54 and 55 gives:

$$P(\text{CH}_3)_3\text{Pb}^+ = \frac{1}{1 + K_f[\text{SCN}^-]} \quad (56)$$

$$P_{(CH_3)_3PbSCN} = \frac{K_f [SCN^-]}{1 + K_f [SCN^-]} \quad (57)$$

The mass balance expressions for the trimethyllead and for the ligand are:

$$[(CH_3)_3Pb]_{\text{total}} = [(CH_3)_3Pb^+] + [(CH_3)_3PbSCN] \quad (58)$$

$$[SCN^-]_{\text{total}} = [SCN^-] + [(CH_3)_3PbSCN] \quad (59)$$

Dividing both sides of Equation 58 by the total trimethyllead concentration yields Equation 60.

$$l = P_{(CH_3)_3Pb^+} + P_{(CH_3)_3PbSCN} \quad (60)$$

Rearrangement and substitution of Equation 60 into Equation 53 yields Equation 61.

$$P_{(CH_3)_3PbSCN} = \frac{\delta_{\text{obs}} - \delta_{(CH_3)_3Pb^+}}{\delta_{(CH_3)_3PbSCN} - \delta_{(CH_3)_3Pb^+}} \quad (61)$$

Substitution of Equation 61 into Equation 55 and then substitution of the resulting equation into Equation 59 gives:

$$[SCN^-] = [SCN]_{\text{total}} - \left(\frac{\delta_{\text{obs}} - \delta_{(CH_3)_3Pb^+}}{\delta_{(CH_3)_3PbSCN} - \delta_{(CH_3)_3Pb^+}} \right) \times [(CH_3)_3Pb]_{\text{total}} \quad (62)$$

K_f and $\delta_{(CH_3)_3PbSCN}$ were evaluated from chemical shift data, over the thiocyanate concentration range 0-1.5 M, using the non-linear least squares curve fitting program KINET. The program was given initial estimates for K_f and $\delta_{(CH_3)_3PbSCN}$. It then calculates $[SCN^-]$ with Equation 62. $P_{(CH_3)_3Pb^+}$ and $P_{(CH_3)_3PbSCN}$ were then calculated by substitution of the estimated K_f and $[SCN^-]$ into Equations 56 and 57. δ_{pred} was then calculated with Equation 53. This procedure is repeated for each data point using the initial estimates of K_f and $\delta_{(CH_3)_3PbSCN}$. The non-linear least squares program then compares each δ_{obs} to δ_{pred} , and adjusts K_f and $\delta_{(CH_3)_3PbSCN}$ to minimize the sum of the squares of the residuals.

The K_f obtained for the $(CH_3)_3PbSCN$ complex by this procedure is 0.381 (± 0.03), where the uncertainty is a linear estimate of the standard deviation. The chemical shift of $\delta_{(CH_3)_3PbSCN}$ is 1.709 ppm. Bertazzi (57) reported a formation constant for the trimethyllead-thiocyanate complex of 631. He determined the constant by anion exchange techniques.

4. Sulfide Complexes of Trimethyllead

The research on the binding of trimethyllead by the sulfide ligand, S^{2-} , is not completed yet, but the work done to date is reported here. The results are of interest because research on the binding of trimethyllead

by glutathione in this laboratory (17) shows that the sulfhydryl group is the strongest organic binding site for trimethyllead.

The binding of trimethyllead by sulfide was investigated by monitoring the chemical shift of the methyl protons of trimethyllead as a function of pH for solutions containing about twice as much ligand as trimethyllead. These conditions were chosen so as to prevent the formation of $((\text{CH}_3)_3\text{Pb})_2\text{S}$ which complicates the studies due to its insoluble nature. The chemical shift of the methyl protons of trimethyllead is presented as a function of pH in Figure 9 for both a solution of trimethyllead perchlorate (open points) and a solution containing trimethyllead perchlorate and sodium sulfide in a ratio of 1/2.46 (solid points). The solutions were made in the same way as in the trimethyllead-sulfite study because of their instability. The two chemical shift titration curves in Figure 9 are different over the entire pH range studied (6.8-13), indicating that complexation of trimethyllead by sulfide is occurring over this pH range.

Of the various models tested for the complexation equilibria, a model which considers the two complexes $(\text{CH}_3)_3\text{PbS}^-$ and $(\text{CH}_3)_3\text{PbSH}$ in addition to the three aqueous species $(\text{CH}_3)_3\text{Pb}^+$, $(\text{CH}_3)_3\text{PbOH}$, and $((\text{CH}_3)_3\text{Pb})_2\text{OH}^+$ provides the best fit to the data. The curve fitting

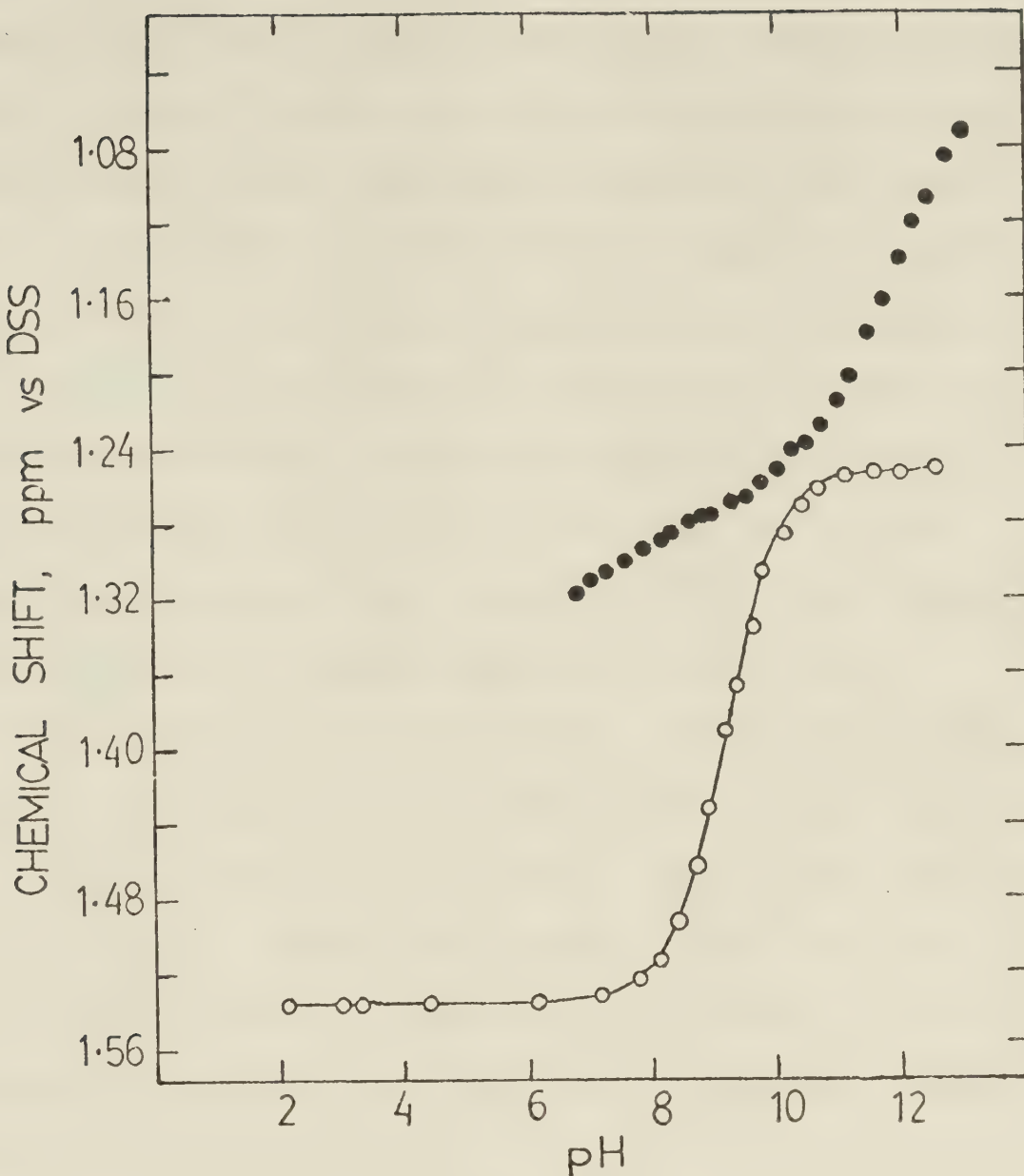


FIGURE 9. pH dependence of the chemical shift of the methyl protons of trimethyllead in an aqueous solution containing 5.00×10^{-3} M trimethyllead perchlorate (open points) and in an aqueous solution containing 5.03×10^{-3} M trimethyllead perchlorate and 0.0124 M sodium sulfide (solid points).

procedure described for the trimethyllead-sulfite system was used, however it has not yet been possible to obtain precise values for the formation constants and chemical shifts of $(\text{CH}_3)_3\text{PbSH}$ and $(\text{CH}_3)_3\text{PbS}^-$. There are experimental problems also in that some precipitate appeared in the nmr tubes after the nmr measurements. This may indicate decomposition of the trimethyllead-sulfide complexes as proposed by Jarvie, Markall and Potter in their mechanism for the formation of tetraalkyllead from trialkyllead solutions containing sulfide(6).

The formation constant of $(\text{CH}_3)_3\text{PbS}^-$ appears to be in the range 10^7 and that of $(\text{CH}_3)_3\text{PbSH}$ in the range 10^4 , consistent with the expectation that trimethyllead forms a stronger complex with sulfide than with the other ligands studied. However, the formation constants are considerably less than for the corresponding methyl-mercury complexes (54).

5. The Phosphate Complex of Trimethyllead

The binding of trimethyllead by phosphate was investigated by monitoring the chemical shift of the methyl protons of trimethyllead as a function of solution conditions. The chemical shift of the trimethyllead protons is presented as a function of pH in Figure 10 for a solution containing trimethyllead perchlorate and di-sodium hydrogen orthophosphate in a ratio of 1/2.7

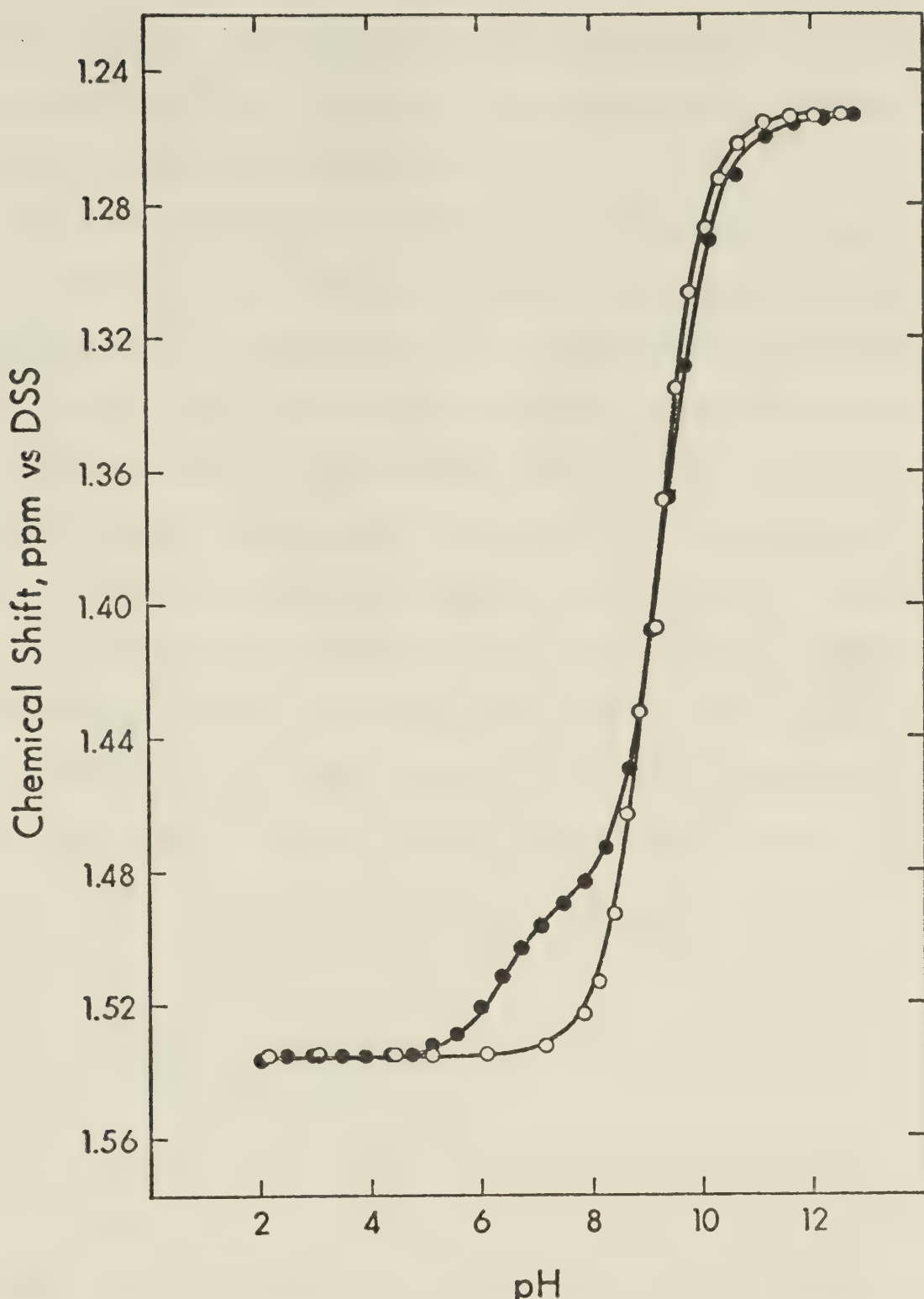


FIGURE 10. pH dependence of the chemical shift of the methyl protons of trimethyllead in an aqueous solution containing 5.00×10^{-3} M trimethyllead perchlorate (open points) and in an aqueous solution containing 5.00×10^{-3} M trimethyllead perchlorate and 0.0135 M di-sodium hydrogen orthophosphate (solid points).

(solid points). For comparison, chemical shift data is also presented for a solution containing only trimethyllead perchlorate (open points).

The two chemical shift titration curves in Figure 10 are different over the pH range 5-12, indicating some complexation of trimethyllead by phosphate over this pH range. Below pH 5, the proton is more successful than the trimethyllead for phosphate, (pK_2 of $H_3PO_4 = 6.71$), so that a large fraction of trimethyllead exists as

$(CH_3)_3Pb^+$ and the ligand as $H_2PO_4^-$. At high pH, hydroxide ion competes with the phosphate for the trimethyllead.

Of the various models tested, the best fit was obtained for a model in which the trimethyllead and phosphate in the form HPO_4^{2-} form a simple one-to-one complex.



$$K_f = \frac{[(CH_3)_3PbHPO_4^-]}{[(CH_3)_3Pb^+] [HPO_4^{2-}]} \quad (64)$$

The formation constant and chemical shift of the trimethyllead-hydrogen phosphate complex were determined from the chemical shift versus pH data by the method described previously for the trimethyllead-sulfite complex. The K_f obtained for $(CH_3)_3PbHPO_4^-$ by this procedure using data covering the pH range 2 to 12.8 is 75.1 ± 3 , where the uncertainty is a linear estimate of the standard

deviation. $\delta_{(CH_3)_3PbHPO_4^-} = 1.435$ ppm was obtained simultaneously. Attempts to fit the observed chemical shift data to models involving other species, for example $(CH_3)_3PbH_2PO_4$ and $(CH_3)_3PbPO_4^{2-}$ in addition to the four species in the model described above gave poor fits. This suggests that at low pH, the phosphate is predominantly in the form $H_2PO_4^-$, and the trimethyllead predominantly $(CH_3)_3Pb^+$. At high pH, the chemical shift data indicate complexation of only a small fraction of the trimethyllead by phosphate, consistent with the formation of $(CH_3)_3PbOH$, and the phosphate is present as PO_4^{3-} ($pK_3 = 12.3$). Consequently, the model represented by Equations 30-33 and 63 and 64 describes the trimethyllead-phosphate system over the pH region 2 to 12.8. The observed and predicted chemical shifts for all the data points are in good agreement (Figure 10).

6. Carbonate Complex of Trimethyllead

The binding of trimethyllead by the carbonate ligand, CO_3^{2-} , was investigated by monitoring the chemical shift of the trimethyllead protons as a function of pH in a solution having a carbonate-to-trimethyllead ratio of 13:1. The large ratio was used to maximize the fraction of trimethyllead complexed. The chemical shift is presented as a function of pH in Figure 11 for both a solution of trimethyllead perchlorate (open points) and a solution containing trimethyllead perchlorate and

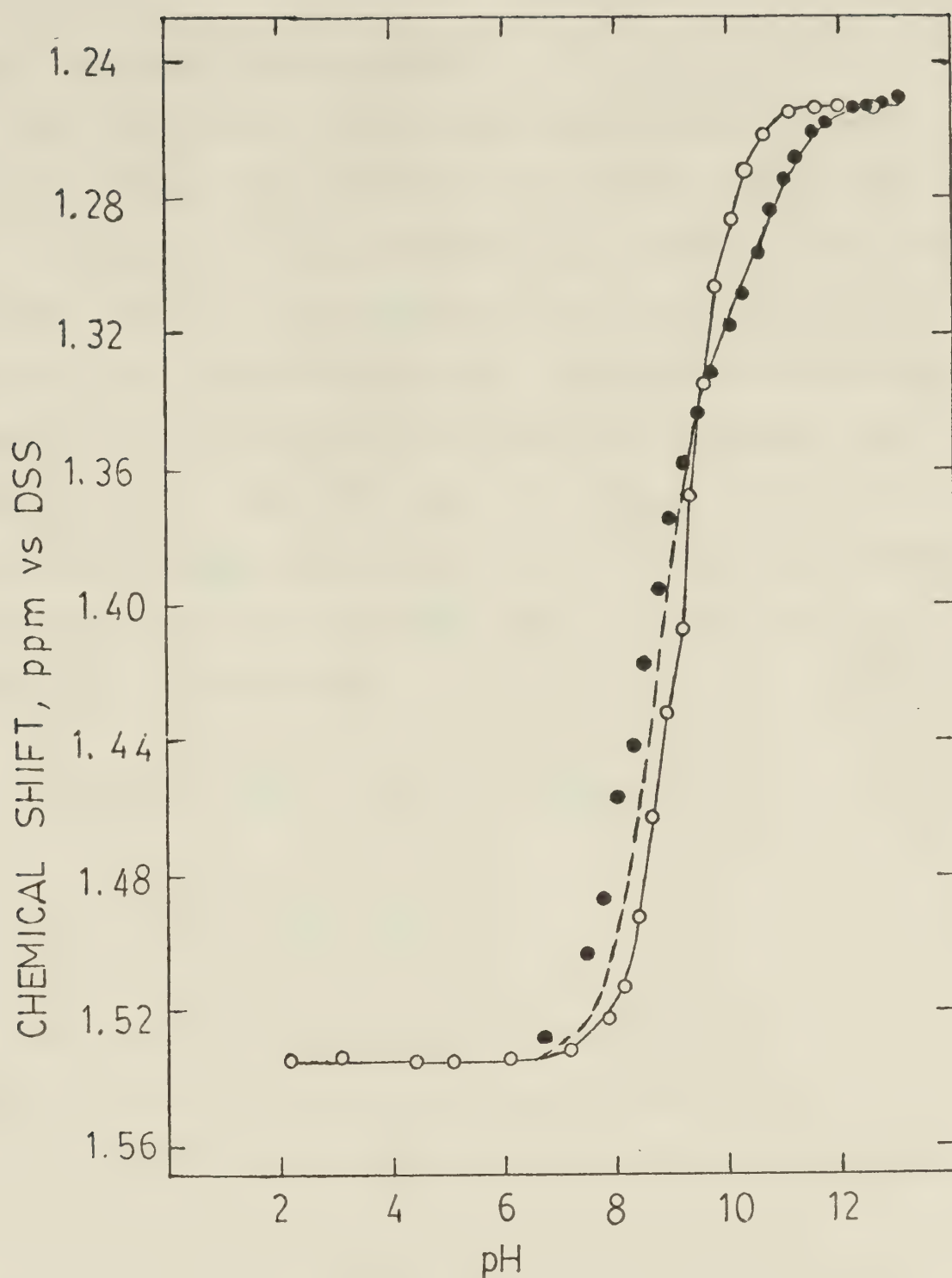
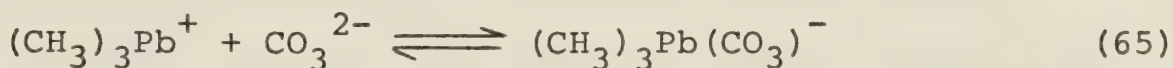


FIGURE 11. pH dependence of the chemical shift of the methyl protons of trimethyllead in an aqueous solution containing 5.00×10^{-3} M trimethyllead perchlorate (open points) and in an aqueous solution containing 5.03×10^{-3} M trimethyllead perchlorate and 0.0650 M sodium carbonate (solid points).

sodium carbonate (solid points).

The two chemical shift titration curves in Figure 11 are different over the pH range 6.7-12, indicating some complexation of trimethyllead by carbonate over this pH range. At high pH, hydroxide ion competes with the carbonate for the trimethyllead, while at low pH protons compete with the trimethyllead for the carbonate (pK_1 and pK_2 of H_2CO_3 are 6.40 and 10.3, respectively). Of the various models tested, the best fit was obtained for a model in which the trimethyllead and carbonate form a simple one-to-one complex.



$$K_f = \frac{[(CH_3)_3Pb(CO_3)^-]}{[(CH_3)_3Pb^+] [CO_3^{2-}]} \quad (66)$$

The formation constant and chemical shift of the trimethyllead-carbonate complex were determined from the chemical shift versus pH data by the method described previously for the trimethyllead-sulfite complex. The K_f obtained for $(CH_3)_3PbCO_3^-$ by this procedure using data covering the pH range 9.2 to 13.0 is 396 ± 32 . A value of 1.347 ppm was obtained simultaneously for $\delta (CH_3)_3PbCO_3^-$. Attempts to fit chemical shift data covering the pH range 6.7 to 9.2 to this model were unsuccessful, with large differences between the observed

and predicted chemical shifts at pH less than 9. In this pH region, the free carbonate is predominantly in the form HCO_3^- , suggesting that the species $(\text{CH}_3)_3\text{PbHCO}_3$ might also be forming. Attempts to fit the observed chemical shift data to a model involving this species in addition to the four species in the model described above were unsuccessful. This suggests that its concentration must be small, or that some other complex is present. Consequently, the model represented by Equations 30-33 and 65 and 66 describes the trimethyllead-carbonate system, only at pH greater than 9.2. The observed and predicted chemical shifts for this pH region are in good agreement (Figure 11). The difference between the predicted chemical shift curve (dashed curve at pH < 9 in Figure 11) and the experimental points indicates that other trimethyllead-carbonate complexes must be forming in this pH range.

7. The Iodide, Bromide, Chloride, and Fluoride Complexes of Trimethyllead.

The binding of trimethyllead by iodide was studied first by monitoring the chemical shift of the methyl protons of trimethyllead as a function of pH in a solution having an iodide-to-trimethyllead ratio of 10:1. The chemical shift titration curve for this solution is different from that of trimethyllead alone at pH < 8,

indicating some complexation of trimethyllead by iodide in this pH region. However, the differences between the curves are small, indicating that iodide interacts only weakly with trimethyllead, and the data could not be fit to obtain a precise formation constant. In order to determine the formation constant, this system was studied by mole ratio experiments at a constant pH, the value of which was chosen so as to maximize the interaction of the ligand with the trimethyllead by minimizing competition from the hydroxide ions for the formation of $(\text{CH}_3)_3\text{PbOH}$. 15 samples whose ratios of sodium iodide to trimethyllead ranged from 0 to 150 were prepared individually at pH 4. In order to keep the ionic strength at 0.3 M for all the samples, the concentration of trimethyllead was reduced to 2.00×10^{-3} M. The chemical shift is presented as a function of $[\text{NaI}]_{\text{total}} / [(\text{CH}_3)_3\text{Pb}]_{\text{total}}$ ratio in Figure 12. The observed chemical shift varies continuously as the ligand to trimethyllead ratio is changed, indicating that the relative amounts of free and complexed trimethyllead are changing. Consequently, the chemical shift of trimethyllead-iodide complex cannot be obtained directly from the data, because in no sample is all the trimethyllead in the iodide-complexed form. The formation constant was calculated for the trimethyllead-iodide complex from the chemical shift data by fitting the data to a model in which the trimethyllead

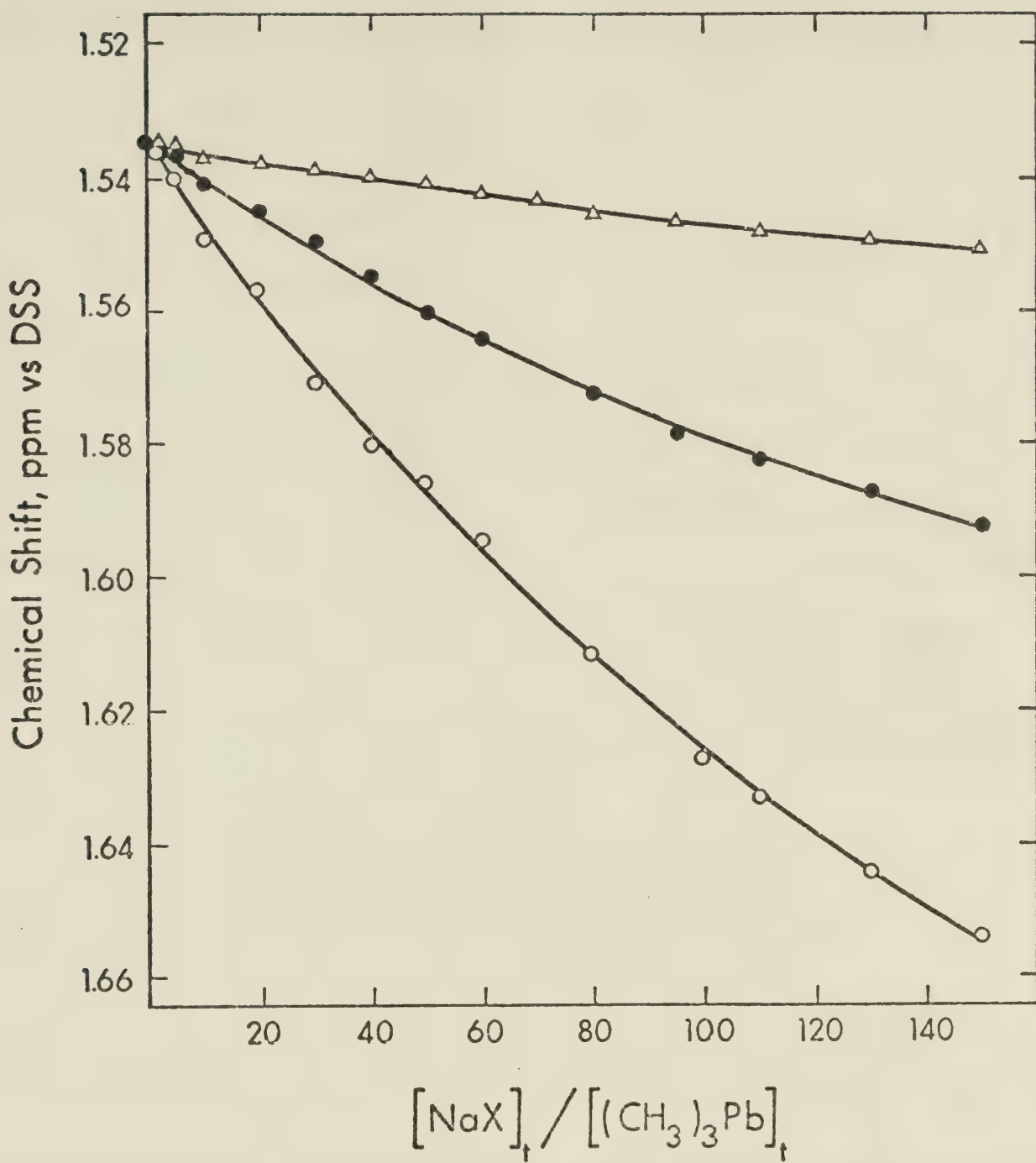
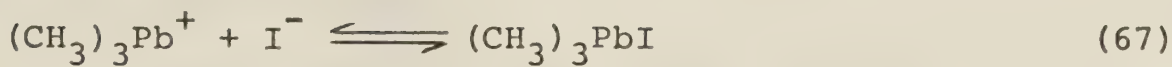


FIGURE 12. The chemical shift of the methyl protons of trimethyllead in aqueous solutions containing 2.00×10^{-3} M trimethyllead perchlorate and sodium halide as a function of the ligand-to-trimethyllead ratio at pH 4.00. Sodium iodide (○), sodium bromide (●), and sodium chloride (Δ).

and iodide form a simple one-to-one complex, $(\text{CH}_3)_3\text{PbI}$.



$$K_f = \frac{[(\text{CH}_3)_3\text{PbI}]}{[(\text{CH}_3)_3\text{Pb}^+][\text{I}^-]} \quad (68)$$

The formation constant and chemical shift of the trimethyllead-iodide complex were determined from the chemical shift versus $[\text{NaI}]_{\text{total}}/[(\text{CH}_3)_3\text{Pb}]_{\text{total}}$ ratio by the method described previously for the trimethyllead-thiocyanate complex. The K_f obtained for $(\text{CH}_3)_3\text{PbI}$ by this procedure is 1.89 (± 0.1), where the uncertainty is a linear estimate of the standard deviation. The chemical shift of $\delta_{(\text{CH}_3)_3\text{PbI}}$ is 1.867 ppm.

The binding of trimethyllead by bromide, chloride, and fluoride was studied by monitoring the chemical shift of the methyl protons of trimethyllead in mole ratio experiments in exactly the same way as just described for the iodide ligand. A pH of 4 was used. The chemical shift is presented as a function of ligand-to-trimethyllead ratio for the bromide and chloride systems in Figure 12. The formation constants for the trimethyllead-bromide and -chloride complexes were calculated from the chemical shift data by fitting the data as described above for the trimethyllead-iodide complex. The values obtained are $K_f = 1.95 (\pm 0.2)$, $\delta_{(\text{CH}_3)_3\text{PbBr}} = 1.692$ ppm for the bromide complex of trimethyllead and

$K_f = 1.22 (\pm 0.4)$, $\delta_{(CH_3)_3PbCl} = 1.595$ ppm for the chloride complex of trimethyllead.

The trimethyllead-fluoride system was also studied by mole ratio experiments, but it was not possible to characterize the complexation equilibria from the chemical shift data. One problem is that a complex precipitates at $[NaF]_{total}/[(CH_3)_3Pb]_{total}$ ratios greater than 70. Also, the chemical shift behavior is difficult to explain. The chemical shift decreases, i.e., the shielding decreases relative to the reference, as the concentration of NaF is increased up to a ligand-to-metal ratio of 20. As the ratio is increased from 20 to 60, the chemical shift increases, and then decreases slightly at ratios greater than 60. A possible explanation is that at pH 4 some of the ligand is present as HF which can etch the glass.

B. Discussion

The chemical shifts and the formation constants of all the complexes studied in this research are summarized in Table 3. The only literature result available for comparison with the formation constants is that reported by Bertazzi for the $(CH_3)_3Pb(SCN)$ complex (57), who obtained a value of 630 by anion exchange techniques. This value is considerably larger than that determined in this work, and much too large to be compatible with the chemical shift data (Figure 8). It is of interest,

however, to compare the formation constants with those for the analogous methylmercury complexes (51,56) which also are listed in Table 3. Unlike the methylmercury complexes the very small change in $J_{^{207}\text{Pb}-^1\text{H}}$ upon formation of $(\text{CH}_3)_3\text{PbOH}$ and carboxylate complexes from $(\text{CH}_3)_3\text{Pb}^+$ in aqueous solution indicate that the lead-207 proton coupling constant is not very sensitive to the complexation of trimethyllead by the ligands. The trimethyllead complexes studied in this work probably form from trigonal bipyramidal $(\text{CH}_3)_3\text{Pb}^+$ by substitution of one H_2O ligand. Their formation constants, with the exception of those for the sulfide and hydrogen sulfide complexes, are small, indicating the affinity of the trimethyllead moiety for these ligands not to be large relative to that for water. The formation constants are much smaller than those for the analogous $\text{CH}_3\text{Hg(II)}$ complexes, which also are listed in Table 3. It is also clear that the relative affinity of $(\text{CH}_3)_3\text{Pb(IV)}$ for oxygen donor groups as compared to sulfur donor groups is much larger than is the case with $\text{CH}_3\text{Hg(II)}$. For example, K_f for the complex $\text{CH}_3\text{Hg}(\text{S}_2\text{O}_3)^-$, in which $\text{CH}_3\text{Hg(II)}$ is sulfur coordinated (58), is 5 orders of magnitude larger than that for $\text{CH}_3\text{Hg}(\text{CO}_3)^-$, whereas K_f for $(\text{CH}_3)_3\text{Pb}(\text{CO}_3)^-$ is 3 times that for $(\text{CH}_3)_3\text{Pb}(\text{S}_2\text{O}_3)^-$. Likewise, K_f for $\text{CH}_3\text{Hg}(\text{SO}_3)^-$, in which $\text{CH}_3\text{Hg(II)}$ is also sulfur coordinated (56,58), is larger than K_f for oxygen-coordinated $\text{CH}_3\text{Hg}(\text{SeO}_3)^-$,

whereas the formation constants for the analogous $(\text{CH}_3)_3\text{Pb}^{(\text{IV})}$ complexes are in the opposite order.

The extent to which the trimethyllead complexes form is very much dependent on pH because of their low formation constants coupled with the competitive formation of $(\text{CH}_3)_3\text{PbOH}$ and $((\text{CH}_3)_3\text{Pb})_2\text{OH}^+$ at high pH and the competitive protonation of those ligands which are conjugate bases of weak acids at low pH. To illustrate, species distribution curves calculated from the formation constants in Table 3 and the equilibrium constants for $(\text{CH}_3)_3\text{PbOH}$ and $((\text{CH}_3)_3\text{Pb})_2\text{OH}^+$ are presented for the trimethyllead-phosphate system in Figure 13, the trimethyllead-thiosulfate system in Figure 14, and the trimethyllead-chloride system in Figure 15. In each case, $(\text{CH}_3)_3\text{PbOH}$ forms at high pH, with the pH at which the trimethyllead is essentially all in this form increasing in the order $\text{Cl}^- < \text{HPO}_4^{2-} < \text{S}_2\text{O}_3^{2-}$, which is the same order in which the formation constants increase. However, the behavior of these three systems at low pH is considerably different. HPO_4^{2-} is the conjugate base of the weak acid H_2PO_4^- , and protonation to form H_2PO_4^- is a more favored process than is complexation by $(\text{CH}_3)_3\text{Pb}^+$. The chemical shift data in Figure 10 indicate no complexation by H_2PO_4^- . Thus there is a correlation between the weak basicity of H_2PO_4^- and its ability to complex $(\text{CH}_3)_3\text{Pb}^+$. Chloride and thiosulfate are extremely weak

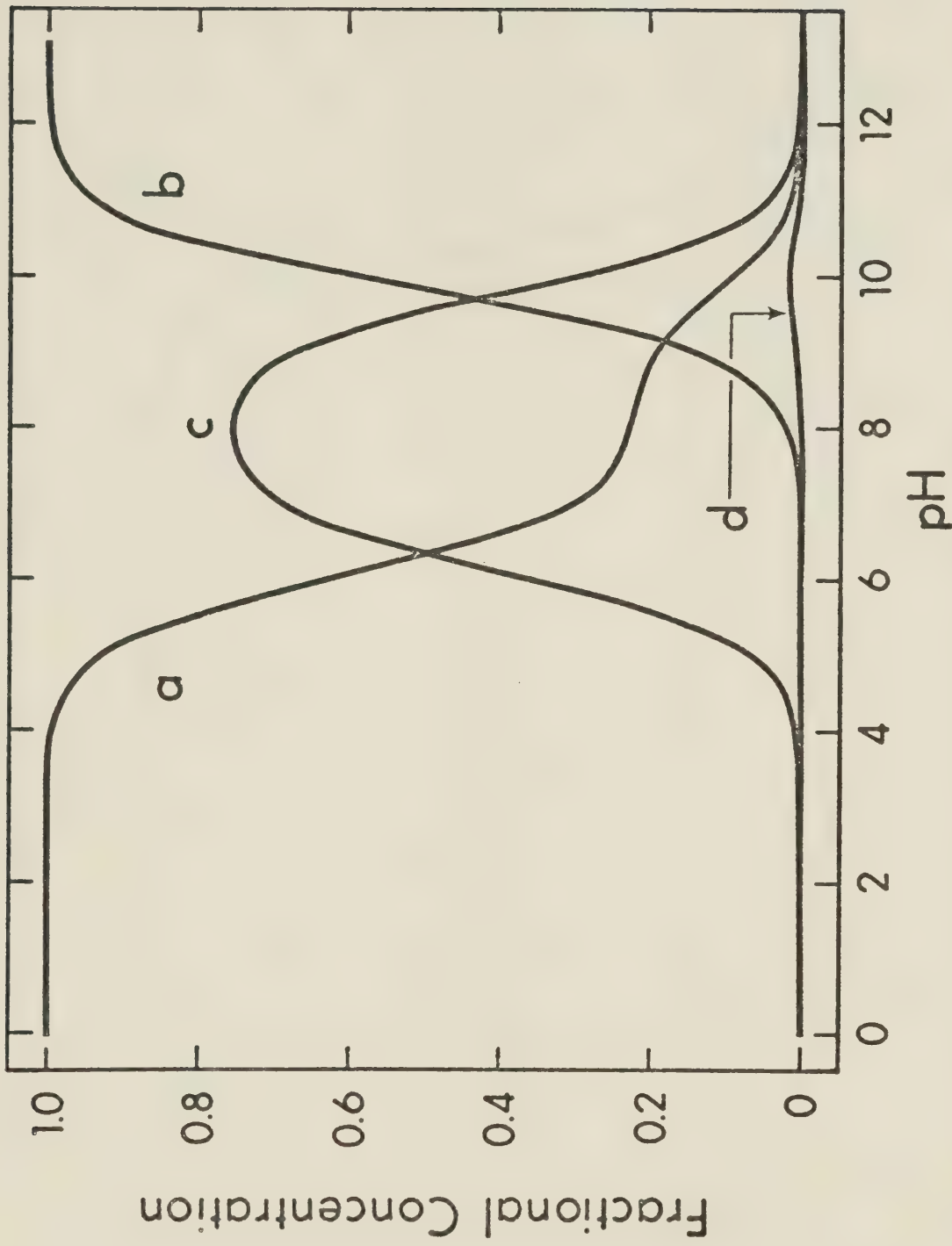


FIGURE 13. pH dependence of the trimethyllead species distribution in an aqueous solution containing 5.00×10^{-3} M trimethyllead perchlorate and 0.0500 M sodium phosphate. $(\text{CH}_3)_3\text{Pb}^+$ (a), $(\text{CH}_3)_3\text{PbOH}^-$ (b), $(\text{CH}_3)_3\text{Pb}(\text{HPO}_4)^{2-}$ (c), and $((\text{CH}_3)_3\text{Pb})_2\text{OH}^+$ (d).

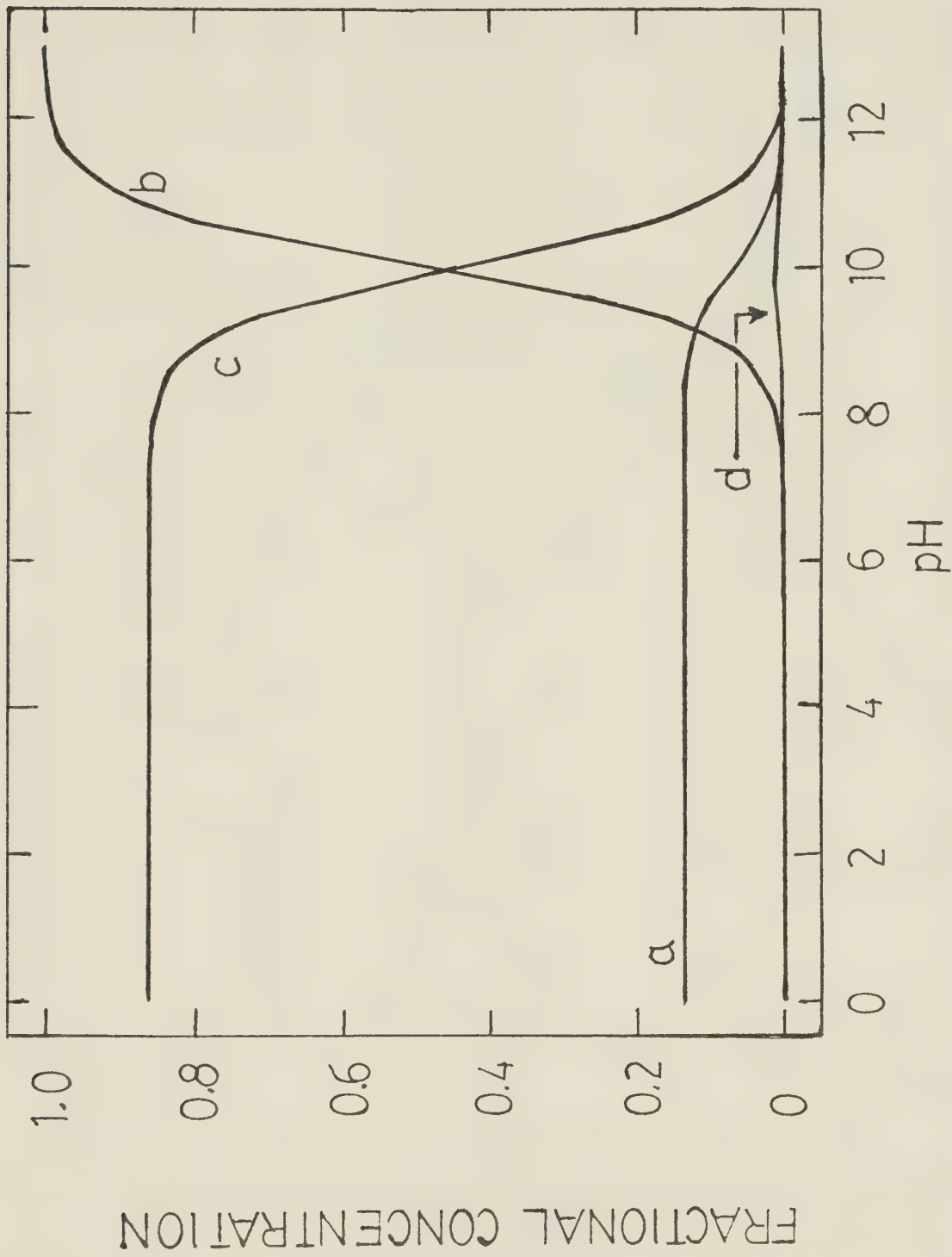
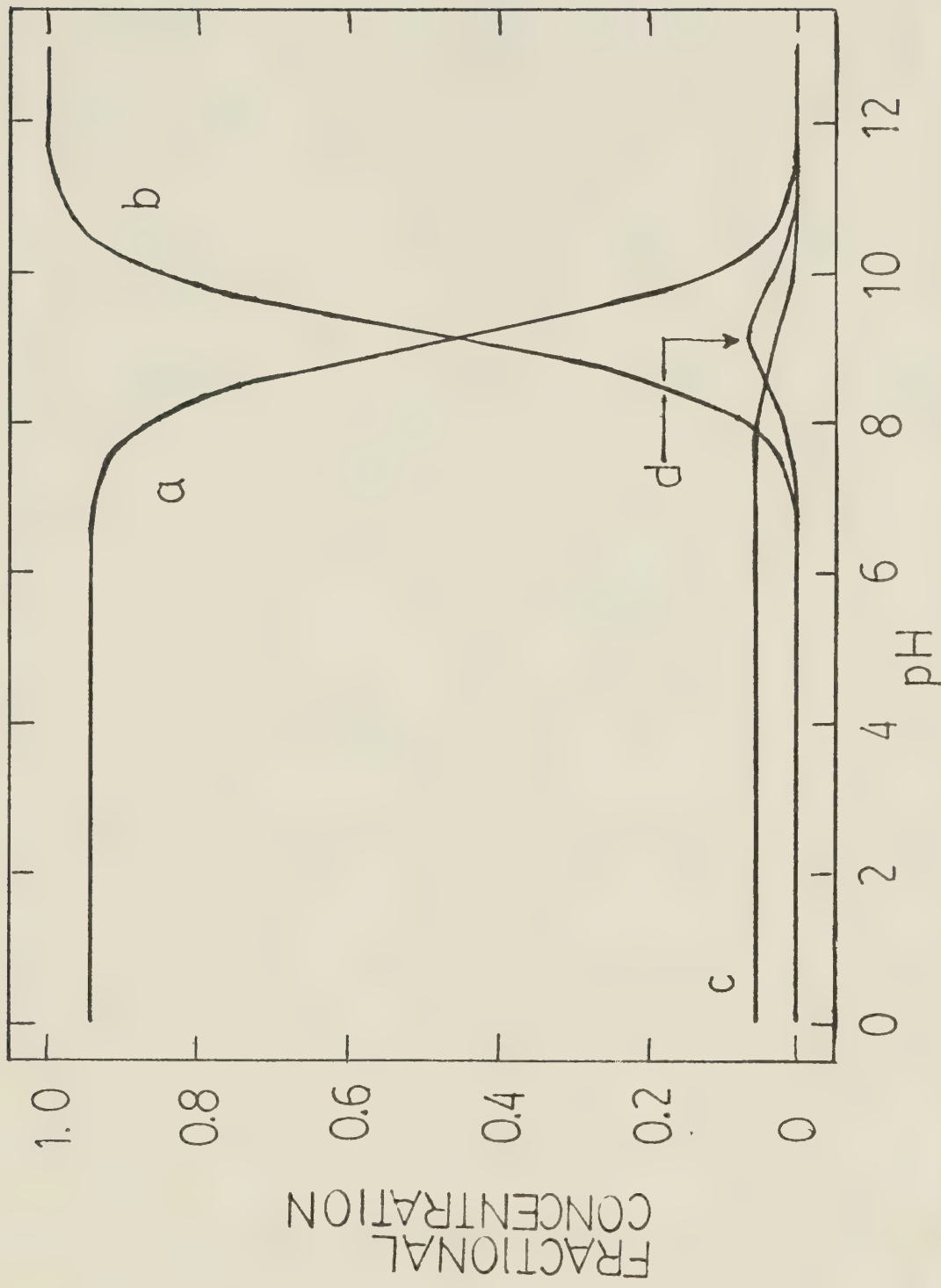
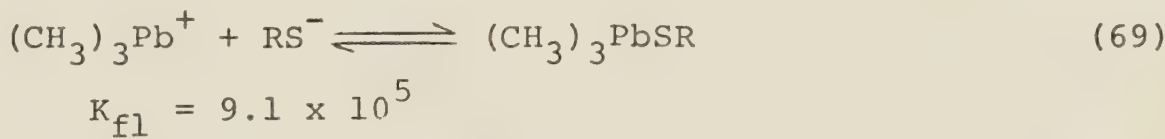


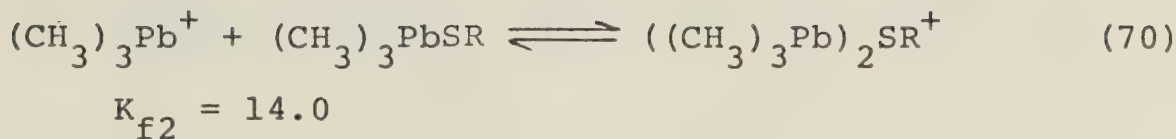
FIGURE 14. pH dependence of the trimethyllead species distribution in an aqueous solution containing 5.00×10^{-3} M trimethyllead perchlorate and 0.0500 M sodium thiosulfate. $(\text{CH}_3)_3\text{Pb}^+$ (a), $(\text{CH}_3)_3\text{PbOH}^-$ (b), $(\text{CH}_3)_3\text{Pb}(\text{S}_2\text{O}_3)^{2-}$ (c), and $((\text{CH}_3)_3\text{Pb})_2\text{OH}^+$ (d).



conjugate bases in the Bronsted sense. Consequently there is no competitive protonation of these ligands and the maximum amount of complex forms at pH < 7-8, where there also is little competitive formation of the hydroxy complexes. The fractional concentration of the complexed form remains constant at pH values less than 7-8. Because there is no competitive protonation of these ligands, relatively large fractions of the $(\text{CH}_3)_3\text{Pb}^+$ can be in these complexed forms even though the K_f 's are small. For example, for chloride the percentage of the trimethyllead in the $(\text{CH}_3)_3\text{PbCl}$ form is 5.7% at low pH for the particular concentrations used in the calculations shown in Figure 15, even though the K_f is only 1.2.

The results in Table 3 together with other results from studies in this laboratory on the coordination chemistry of trimethyllead (17,49) indicate that trimethyllead does not show a strong preference for any particular type of donor group. The largest formation constants appear to be with the deprotonated sulfhydryl groups of organic thiol ligands (17). For example, the model for trimethyllead and mercaptoethanol complexes and their formation constants are (17):





This is of particular interest with respect to the chemistry of trimethyllead in biological fluids, where there are an abundance of potential ligands, including carboxylate groups, carbonate, inorganic and organic phosphate and chloride in addition to the sulphydryl groups of peptides and proteins. Because of the different pH dependence of the extent to which the various complexes form and the relative abundances of the different ligands, the formation constants predict that, at physiological pH, there will be a significant fraction of $(CH_3)_3Pb(IV)$ complexed even by those ligands having small formation constants. To illustrate, the pH dependence of the fractional concentrations of the various trimethyllead species has been calculated for solutions containing 2-mercaptoethanol, phosphate, and trimethyllead (Figures 16 and 17) and for a solution containing 2-mercaptoethanol, chloride, and trimethyllead (Figure 18). Even though the K_f 's for the $(CH_3)_3Pb(HPO_4)^-$ and $(CH_3)_3PbCl$ complexes are considerably smaller than those for the 2-mercaptoethanol complexes, some $(CH_3)_3Pb(HPO_4)^-$ and some $(CH_3)_3PbCl$ form because of the competitive protonation of the sulphydryl ligand. This situation is in marked contrast to that for $CH_3Hg(II)$, which shows such an extreme affinity for sulphydryl ligands that in

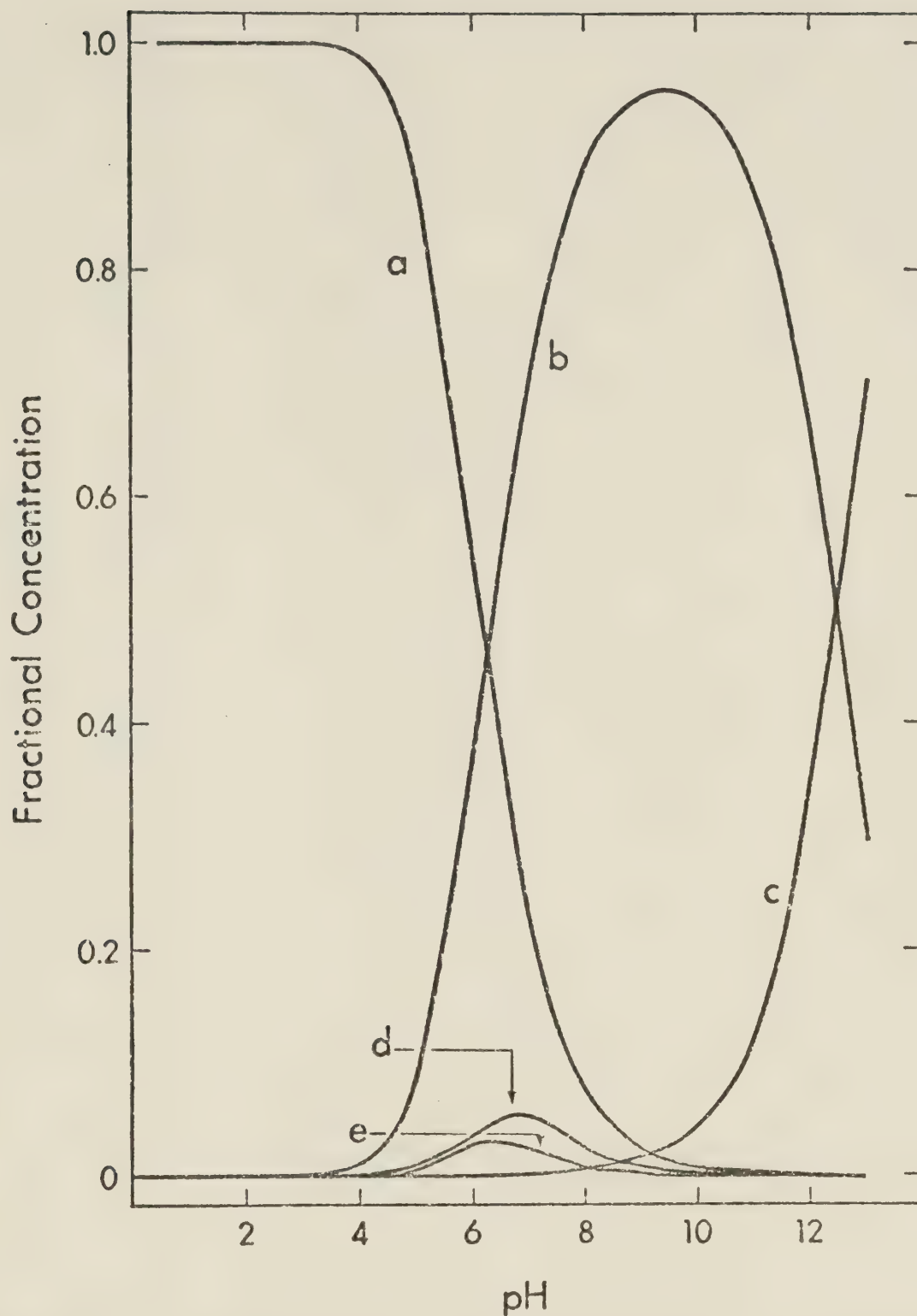


FIGURE 16. pH dependence of the distribution of trimethyllead among its various forms in an aqueous solution containing trimethyllead perchlorate, 2-mercaptopethanol and sodium phosphate, each at a total concentration of 5.00×10^{-3} M. $(\text{CH}_3)_3\text{Pb}^+$ (a), $(\text{CH}_3)_3\text{Pb}(\text{SCH}_2\text{CH}_2\text{OH})$ (b), $(\text{CH}_3)_3\text{PbOH}$ (c), $(\text{CH}_3)_3\text{Pb}(\text{HPO}_4)^-$ (d), and $((\text{CH}_3)_3\text{Pb})_2\text{SCH}_2\text{CH}_2\text{OH}^+$ (e).

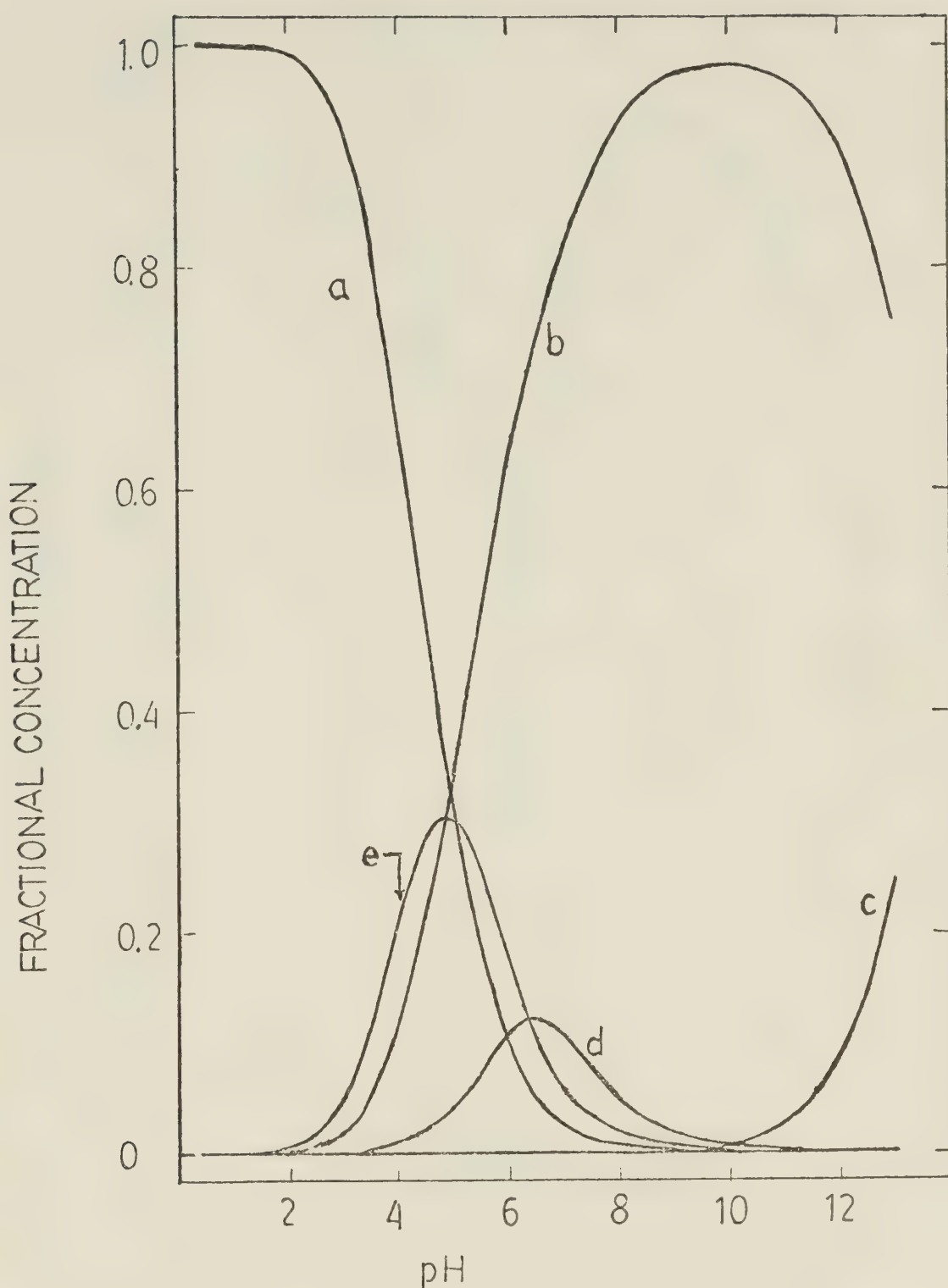


FIGURE 17. pH dependence of the distribution of trimethyllead among its various forms in an aqueous solution containing trimethyllead perchlorate, 2-mercaptoethanol and sodium phosphate, each at a total concentration of 0.100 M. $(\text{CH}_3)_3\text{Pb}^+$ (a), $(\text{CH}_3)_3\text{Pb}^-(\text{SCH}_2\text{CH}_2\text{OH})$ (b), $(\text{CH}_3)_3\text{PbOH}$ (c), $(\text{CH}_3)_3\text{Pb}(\text{HPO}_4)^-$ (d), and $((\text{CH}_3)_3\text{Pb})_2\text{SCH}_2\text{CH}_2\text{OH}^+$ (e).

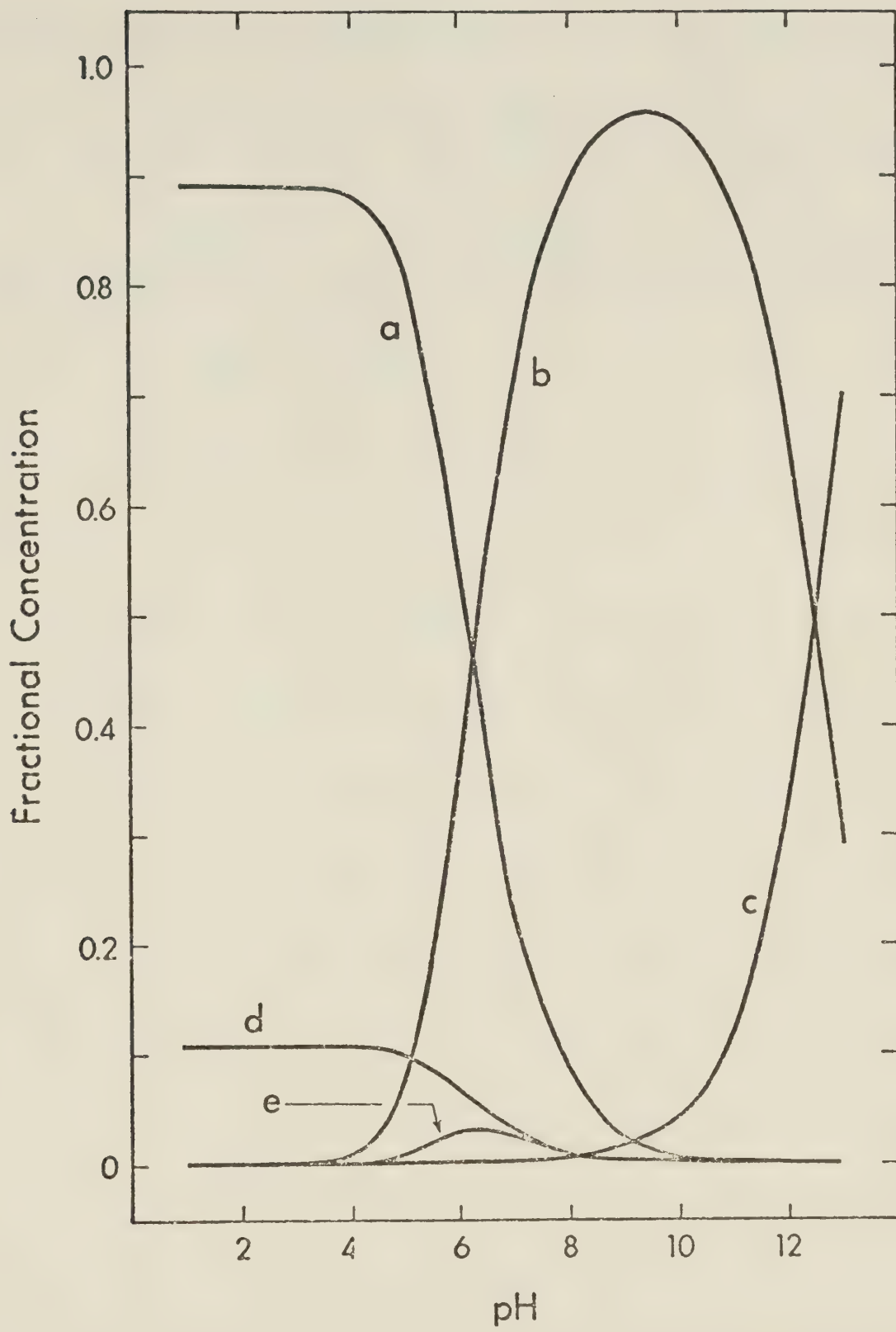


FIGURE 18. pH dependence of the distribution of trimethyllead among its various forms in an aqueous solution containing 5.00×10^{-3} M trimethyllead perchlorate and 2-mercaptoethanol and 0.100 M sodium chloride.

$(CH_3)_3Pb^+$ (a), $(CH_3)_3Pb(SCH_2CH_2OH)$ (b), $(CH_3)_3^-$
 $PbOH$ (c), $(CH_3)_3PbCl$ (d), and $((CH_3)_3Pb)_2SCH_2CH_2OH^+$ (e)

biological systems essentially all of the $\text{CH}_3\text{Hg(II)}$ is assumed to be complexed by the sulfhydryl groups of peptides and proteins (58). The presence of even a small fraction of $(\text{CH}_3)_3\text{Pb(IV)}$ as $(\text{CH}_3)_3\text{PbCl}$ is of particular interest because this complex has electroneutrality and most likely is lipid soluble.

BIBLIOGRAPHY

1. J. E. Cremer, Brit. J. Ind. Med., 16, 191 (1959).
2. J. E. Cremer, Occ. Health Rev., 17, 14 (1965).
3. P. T. S. Wong, Y. K. Chau, and P. L. Luxon, Nature, 253, 263 (1975).
4. G. J. M. Van der Kerk, International Conference on Lead, 3, Pergamon Press, London, 1969. p. 409.
5. Lead. Airborne lead in perspective, 18 (Natn. Acad. Sci. Washington, D.C., 1972).
6. A. W. P. Jarvie, R. N. Markall, and H. R. Potter, Nature, 255, 217 (1975).
7. H. J. Haupt, F. Huber, and J. Gmehling, Z. anorg. allg. Chem., 390, 31 (1972).
8. J. Gmehling, thesis, Univ. Dortmund (1973), cited in U. Schmidt and F. Huber, Nature, 259, 157 (1976).
9. U. Schmidt and F. Huber, Nature, 259, 157 (1976).
10. W. P. Ridley, L. J. Dizikes, and J. M. Wood, Science, 197, 329 (1977).
11. N. I. Sax, "Dangerous Properties of Industrial Materials," Reinhold Publishing Corporation, New York, N.Y., 1968. p. 865.
12. L. W. Sanders, Arch. Environ. Health, 8, 270 (1964).
13. H. Shapiro and F. W. Frey, "The Organic Compounds of Lead," Interscience Publishers, New York, N.Y., 1968, p. 17-21.
14. L. H. Miller, Ind. Med. And Surg., 28, 144 (1959).
15. P. R. Boyd, Lancet, 1, 181 (1957).
16. K. V. Kitzmiller, J. Cholak, and R. A. Kehoe, Arch. Indust. Hyg. Occup. Med., 10, 312 (1954).
17. S. Backs, unpublished results, University of Alberta, 1977.
18. J. E. Cremer, Ann. Occupational Hyg., 3, 226 (1961).

19. A. Polis, Ber., 20, 716 (1887).
20. A. Polis, Ber., 20, 3331 (1887).
21. A. Polis, Ber., 21, 3424 (1888).
22. R. J. H. Clark, A. G. Davies, and R. J. Puddephatt, J. Am. Chem. Soc., 90, 6923 (1968).
23. N. A. Matwiyoff and R. S. Drago, Inorg. Chem., 3, 337 (1964).
24. H. C. Clark, R. J. O'Brien, and J. Trotter, Proc. Chem. Soc., 85 (1963).
25. Y. M. Chow and D. Britton, Acta Cryst., B27, 856 (1971).
26. R. S. Tobias, Organometal. Chem. Rev., 1, 93 (1966).
27. H. Kriegsmann, H. Hoffmann, and S. Pischtschan, Z. Anorg. Allgem. Chem., 315, 283 (1962).
28. R. Okawara and K. Yasuda, J. Organometal. Chem., 1, 356 (1964).
29. K. Yasuda and R. Okawara, J. Organometal. Chem., 3, 76 (1965).
30. H. C. Clark and R. J. O'Brien, Inorg. Chem., 2, 740 (1963).
31. R. Okawara, B. J. Hathaway, and D. E. Webster, Proc. Chem. Soc., 13 (1963).
32. B. J. Hathaway and D. E. Webster, Proc. Chem. Soc., 14 (1963).
33. H. C. Clark and R. J. O'Brien, Inorg. Chem., 2, 1020 (1963).
34. R. Okawara, D. E. Webster, and E. G. Rochow, J. Am. Chem. Soc., 82, 3287 (1960).
35. R. Okawara and M. Ohara, J. Organometal. Chem., 1, 360 (1964).
36. M. J. Janssen, G. J. M. van der Kerk, and J. G. A. Luijten, Rec. Trav. Chim., 82, 90 (1963).
37. G. J. M. van der Kerk, J. G. A. Luijten, and M. J. Janssen, Chimia, 16, 10 (1962).

38. M. J. Janssen, J. G. A. Luijten, and G. J. M. van der Kerk, *J. Organometal. Chem.*, 1, 286 (1964).
39. Y. Kawasaki, T. Tanaka, and R. Okawara, *Bull. Chem. Soc. Japan*, 37, 903 (1964).
40. J. G. A. Luijten, M. J. Janssen, and G. J. M. van der Kerk, *Rec. Trav. Chim.*, 81, 203 (1962).
41. P. Goggin, D. Phil. thesis, Oxford, 1960, p. 156, cited in I. R. Beattie, *Quart. Rev.*, 17, 382 (1963).
42. D. L. Rabenstein and C. A. Evans, unpublished results, University of Alberta, 1977.
43. A. J. Downs and I. A. Steer, *J. Organometal. Chem.*, 8, p. 21 (1967).
44. G. D. Shier, Ph.D. thesis, University of Illinois, 1964, cited in G. D. Shier and R. S. Drago, *J. Organometal. Chem.*, 6, 359 (1966).
45. R. G. Pearson, "Hard and Soft Acids and Bases," Benchmark Papers in Inorganic Chemistry, Dowden, Hutchinson, and Ross, Inc., Stroudsburg, Pennsylvania, 1973.
46. J. R. Holmes and H. D. Kaesz, *J. Am. Chem. Soc.*, 83, 3903 (1961).
47. G. D. Shier and R. S. Drago, *J. Organometal. Chem.*, 6, 359 (1966).
48. T. L. Sayer, Ph.D. thesis, University of Alberta, 1976.
49. T. L. Sayer, S. Backs, C. A. Evans, E. K. Millar, and D. L. Rabenstein, *Can. J. Chem.*, 55, 3255 (1977).
50. G. Calingaert, F. J. Dykstra, and H. Shapiro, *J. Am. Chem. Soc.*, 67, 190 (1945).
51. S. Libich and D. L. Rabenstein, *Anal. Chem.*, 45, 118 (1973).
52. A. I. Vogel, "Quantitative Inorganic Analysis," 3rd ed., John Wiley and Sons Inc., New York, N.Y., 1961.
53. J. L. Dye and V. A. Nicely, *J. Chem. Ed.*, 48, 443 (1971).

54. G. Schwarzenbach and M. Schellenberg, *Helv. Chim. Acta*, 48, 28 (1965).
55. D. L. Rabenstein, C. A. Evans, M. C. Tourangeau, and M. T. Fairhurst, *Anal. Chem.*, 47, 338 (1975).
56. D. L. Rabenstein, M. C. Tourangeau, and C. A. Evans, *Can. J. Chem.*, 54, 2517 (1976).
57. N. Bertazzi, *Z. anorg. allg. Chem.*, 410, 316 (1974).
58. D. L. Rabenstein, *Acc. Chem. Res.*, in press.

B30216